Bmi1+ cells and maturation of murine corneal epithelium

Pro Gradu

Bideep Shrestha

University of Helsinki
Faculty of Biological and Environmental Sciencees
Department of Molecular Biosciences
General Biochemistry
August 2020

Tiedekunta – Fakultet – Faculty Faculty of biological and Environmental Sciences	Koulutusohjelma – Utbildingsprogram – Degree Programme Molecular Biosciences	
Tekijä – Författare – Author Bideep Shrestha		
Työn nimi – Arbetets titel – Title *Bmi1+* cells and maturation of murine corneal epithelium.		
Oppiaine/Opintosuunta – Läroämne/Studieinriktning – Subject/Study track General Biochemistry		
Työn laji – Arbetets art – Level Master's thesis	Aika – Datum – Month and year August 2020	Sivumäärä – Sidoantal – Number of pages 61

Tiivistelmä – Referat – Abstract

Cornea is transparent layer of cells lying in front of lens. The corneal epithelium, a squamous epithelium, covers the ocular surface and ensures proper vision by preserving the integrity of the eye. Corneal epithelium is renewed continuously throughout life from a pool of stem cells (SC). There are still conflicting theories about the localization of stem cells required for the growth, renewal and maintenance of the corneal epithelium. Previous studies demonstrated that the limbus, located in the periphery of the cornea, serves as the stem cell niche (SCN) in adults. However, contrasting evidence from clonal analysis proposes that, in early postnatal life, renewal is fuelled by SCs located in the basal layer of the central cornea. There are alternate patterns of renewal in young and adult mouse cornea and that there is an important, transitional time frame called cornea maturation, when the adult patterns of gene expression, cell dynamics and tissue renewal are established. In the cornea, solid SC markers are still missing, yet studies on human limbal cells have suggested *Bmi1* and C/EBPδ as limbal SC markers. There are, indeed, long-lived SCs in the central cornea and that the gene *Bmi1* plays a role in these central corneal SCs. However, the physiological importance of these *Bmi1+* cells remains obscure. The main aim of this project is to understand the fate and dynamics of these *Bmi1+* cells and study the chronology of maturation of the cornea. In this study, I have also tried to correlate the growth of eye size with proliferation of corneal epithelial cells

This study was conducted using few different kinds of transgenic mice (Mus musculus). To study the fate of *Bmi1+* cells, two different mouse lines were crossed: *Bmi1-CreER* and *ROSA26-LacZ.* Mice carrying both alleles were used for lineage tracing experiments. Moreover, Hematoxylin-eosin staining was used to follow the eye morphology. Immunohistochemistry was performed to follow the chronology of maturation of the cornea, proliferation of corneal epithelial cells and the location of *Bmi1+* cells in corneal epithelium.

From this study, we can propose that cornea maturation is completed by the time of eyelid opening, which take place two weeks after birth. *Krt19* is perfect for studying the chronology of the corneal epithelium, immunostaining of *Krt19* separates the territory of limbus from central cornea enabling to distinguish limbus distinctly. Proliferating cells reside in basal layer of cornea. *Bmi1+* cells found throughout the basal layer of the cornea that locally renews the corneal epithelium concluding *Bmi1+* cells as the progenitor cells.

Avainsanat – Nyckelord – Keywords
Cornea, Corneal epithelium, Limbus, Stem cells, *Bmi1*

Ohjaaja tai ohjaajat – Handledare – Supervisor or supervisors
Frederic Michon

Säilytyspaikka – Förvaringställe – Where deposited
Viikki Campus library
Helsingin yliopiston kirjasto, Helsingfors universitets bibliotek, Helsinki University Library

Muita tietoja – Övriga uppgifter – Additional information

Table of Contents

List of Figures

List of Table

LIST OF ABBREVIATIONS

AMP	Amplifier
ACDBio	Advanced Cell Diagnostics
BSA	Bovine Serum Albumin
BV	Blood Vessel
CE	Corneal Epithelium
CESCs	Corneal Epithelium Stem Cells
DAB	3, 3′ diaminobenzidine tetrahydrochloride
DMSO	Dimethyl sulfoxide
DNA	Deoxyribose nucleic acid
EDTA	Ethylene diamine tetra acetic acid
ESCs	Embryonic stem Cells
GA	Glutaraldehyde
HH	Hamburger and Hamilton
KD	Kilo Dalton
Krt	Keratin
LESCs	Limbal Epithelial Stem Cells
MSCs	Multipotent Stem Cells
PBS	Phosphate-buffered saline
PBST	Phosphate-buffered saline with Tween® 20
PCR	Polymerase chain reaction
PFA	Paraformaldehyde
RNA	Ribose nucleic acid
SCN	Stem cell niche
SCs	Steam Cells
TAC	Transit Amplifying Cell
TDCs	Terminally Differentiated Cells
UV	Ultraviolet

ORIGINAL PUBLICATION.

- Kalha, S., Shrestha, B., Sanz Navarro, M., Jones, K. B., Klein, O. D., and Michon, F. (2017). *Bmi1+* progenitor cell dynamics in murine cornea during homeostasis and wound healing. *Stem Cells (Dayton, Ohio)*, doi:10.1002/stem.2767.

1. INTRODUCTION

The cornea is the first line of defense for camera-type eyes. While the corneal structure is similar in most organisms across camera-type eye evolution, here the murine eye will be used for the study. Its cornea is a dome shaped transparent layer of cells lying in front of lens. Stratified epithelium, stroma and endothelium are the three major layers of mature cornea. All parts of the cornea (epithelium, stroma and endothelium) are avascular. Only the mesenchyme below the limbus, a ring-shaped structure at the periphery of the cornea, and serving as stem cell niche, contains some blood vessels. The corneal epithelium is a 5-7 cells thick layer of non-keratinized, stratified squamous cells, which is separated from the underlying stroma. The latter is formed of highly coordinated collagen fibers, secreted by few keratocytes. Finally, the most internal layer is the endothelium, a single cell layer (Dhouailly et al., 2014). The cells in both stroma and endothelium are derived from the neural crest cells, which migrate between the lens and the forming corneal epithelium. My study focused on the chronology and maturation of corneal epithelial layer in post-natal and young mice.

A member of the Polycomb repressive complex 1 (PRC1), *Bmi1* is essential in various biological processes such as embryonic development, organ formation, stem cell stabilization and differentiation (Valiente-Alandi et al., 2015). In the crypt of the small intestine, there is a population of self-renewing and multipotent adult stem cells, which is capable of supporting the regeneration of intestinal epithelium, and *Bmi1* is a molecular marker for that cell population (Yan et al., 2012). In human, *Bmi1* is expressed in the area where corneal stem cells were identified, which is called limbus (Barbaro et al., 2007).

Some studies showed that corneal epithelium stem cells (CESC) solely reside in the basal layer of the limbal epithelium, a transitional zone attached with the conjunctiva (Collinson et al., 2002). While some studies showed that CESCs, needed for the normal renewal of the epithelium, are scattered throughout its basal layer and stem cells residing in limbal epithelium contribute only in case of wound healing (Majo et al., 2008b). Stem cells present in the basal layer of the epithelium give rise to the transient amplifying (TA) cells, which afterward differentiate into new daughter cells and they are pushed into the suprabasal layers to replace the dead cells (Dhouailly et al., 2014). However, there are still conflicting theories about the localization of stem cells required for the growth, renewal and maintenance of the corneal epithelium. The main aim of this study is to know the localization and fate of *Bmi1* and to investigate the involvement of *Bmi1*+ cells in maturation and proliferation of corneal epithelium. The

literature review will first discuss about the stem cells and stemness of cell. Then it will provide insight in known facts about maturation and maintenance of the corneal epithelium.

The result section will represent the chronology and maturation of corneal epithelium along with the age of animal. The result also demonstrates the relation between growth in eye size and proliferation of corneal epithelium. Importantly, the result section also has shown the localization and the fate of the *Bmi1+* in the corneal epithelium specially within the limbus by taking advantages of two different genetically modified mouse model *Bmi1*$^{CreERT/wt}$*;R26R-LacZ* and genetic fate mapping technique.

2. LITERATURE REVIEW

2.1. Stem cells

Since 19th century in biological and medical science, it has been observed that the tissues have diverge efficiency to regenerate and recognize tissues that can self-renew during the organism's period of living. The concept of existence of stem cells (SCs) were emerged from the self-renewal capacity of the self-renewing tissues. By that time, the approach of SCs and tissue self-renewal has been thoroughly studied together.

Stemness of a cell is defined as the ability of that cell to reconstruct a reliant tissue throughout the life cycle of an organism. SCs are a subset of the undifferentiated cells that are present throughout the life span from embryonic stage to adult stage. These group of cells have the unique capability to self-renew and restock themselves and the potential to differentiate into different types of mature cells. These are the major two characteristics of SCs; self-renewing and potency which play important role in organogenesis in embryonic stage and tissue regeneration in adult stages. In many cases, the stem cell does not divide itself, it remains in the niche while its sister cell leaves the niche and differentiates. In some of the organs such as gut, epidermis, bone marrow, SCs regularly replace worn-out cells and repair damaged tissues while in other organs such as heart and prostate, SCs divide only in response to stress or when organ need to be repaired.

Based on the sources, SCs are divided into two major divisions that are embryonic SCs and adult SCs. The cells which are derived from the inner cell mass of mammalian blastocysts are known as Embryonic stem (ES) cells, these cells differentiate into cells of all three germ layers and also maintains the pluripotency since these cells have the capability to nurture for forever (Martin, 1981). Once the organs are matured, the SCs found in those are known as Adult SCs. These SCs usually involve in replacing and repairing tissues of that particular organ and can form only a subset of cell types (Barker et al., 2010).

Classification to SCs can be done according to their potency, resembling the range of lineages into which they can differentiate. All cell lineages are derived from the totipotent SCs, these cells are most undifferentiated cells which are found in the first stage of the development. The inner cell mass forms the three primary germ layers (ectoderm, mesoderm, endoderm), this cell mass is present in the blastocyst

and the cells composing the inner cell mass are pluripotent SCs commonly known as embryonic SCs. The expression of transcription factors such as *NANOG*, *Sox2*, *Oct4* and *Rex-1* show that the embryonic stem cells are undifferentiated (Hambiliki et al., 2012)which can be expanded *in vitro* in specific culture medium (Evans & Kaufman, 1981) (Williams et al., 1988). In adult tissues such as bone marrow stroma and also in corneal stroma, there is presence of multipotent stem cells which have ability to differentiate into multiple cell types within the tissue (Beltrami et al., 2003)(Friedenstein et al., 1976)(Polisetty, Fatima, Madhira, Sangwan, & Vemuganti, 2008). When cultured in specific culture conditions, MSCs adhere to the culture plate generating colonies which express specific markers such as *CD73, CD90* and *CD105* (Dominici et al., 2006) and have ability to differentiate into osteogenic, chondrogenic and adipogenic lineages (Hass et al., 2011). MSCs of the limbal stroma which express *Krt3, Krt12* and *Krt15* have ability to transdifferentiate into corneal epithelial cells (Katikireddy et al., 2014). In human ocular surface, conjunctival keratinocytes and goblet cells are renewed from shared oligopotent progenitor cells (Pellegrini et al., 1999). Similar studies showed that oligopotent keratinocytes were able to generate both corneal and conjunctival colonies (Majo et al., 2008a).

2.2. Cornea

The cornea is the outer most transparent layer of the eye being our window to the world. It is essential to maintain the transparency of corneal tissue for vision. Being the outer most layer, cornea is also the first line of defence for our eye, protecting eye from being damaged by chemicals, radiations, infection and other physical traumas. Since cornea is exposed to the outer world directly, it is more prone to get damage thus needs continues maintenance throughout the lifetime. Like other epithelia, the epithelium of the cornea is maintained by SCs.

2.2.1. Structure and function of cornea

Cornea is the front-line defence of the eye just lying in front of the lens (Figure 1A). The main function of the cornea is to protect eye from the outer world's hazard, and to transmit and refract light providing to the lens. The matured cornea consists of an avascular, highly aligned collagenous stromal tissue covered on top with a self-renewing stratified non-keratinizing epithelial cell layer, and at the bottom with a single cell layered endothelium (Figure 1B). In human, approximately 10% of the total thickness of the anterior cornea is composed of 5-7 layered, non-keratinized, squamous epithelium. Corneal epithelium is separate out from other 90% of the cornea which contains dense keratocyte and

collagens yet transparent avascular stroma by Bowman's layer (Figure 1B). In human, bowman's layer is prime which is thought to absorb major ultraviolet radiations. Cornea is linked to conjunctiva and then to the palpebral skin through a transitional zone known as the limbus (Figure 1A and 1C) (Kolozsvári et al., 2002). Descemet's membrane is another basement membrane that partition stroma from endothelial mono-cell layer (Haustein, 1983). This basement membrane helps to transport nutrients and water to and from the stroma to prevent corneal oedema and maintain optimal hydration (Nick Di Girolamo, 2011). Cornea is a transparent cells layer allowing light to pass through it to retina via lens. The evenly association of collagen fibrils with extremely uniform diameters and interfibrillar distances in the central cornea is one of the major factors for corneal transparency (Hay, 1980).

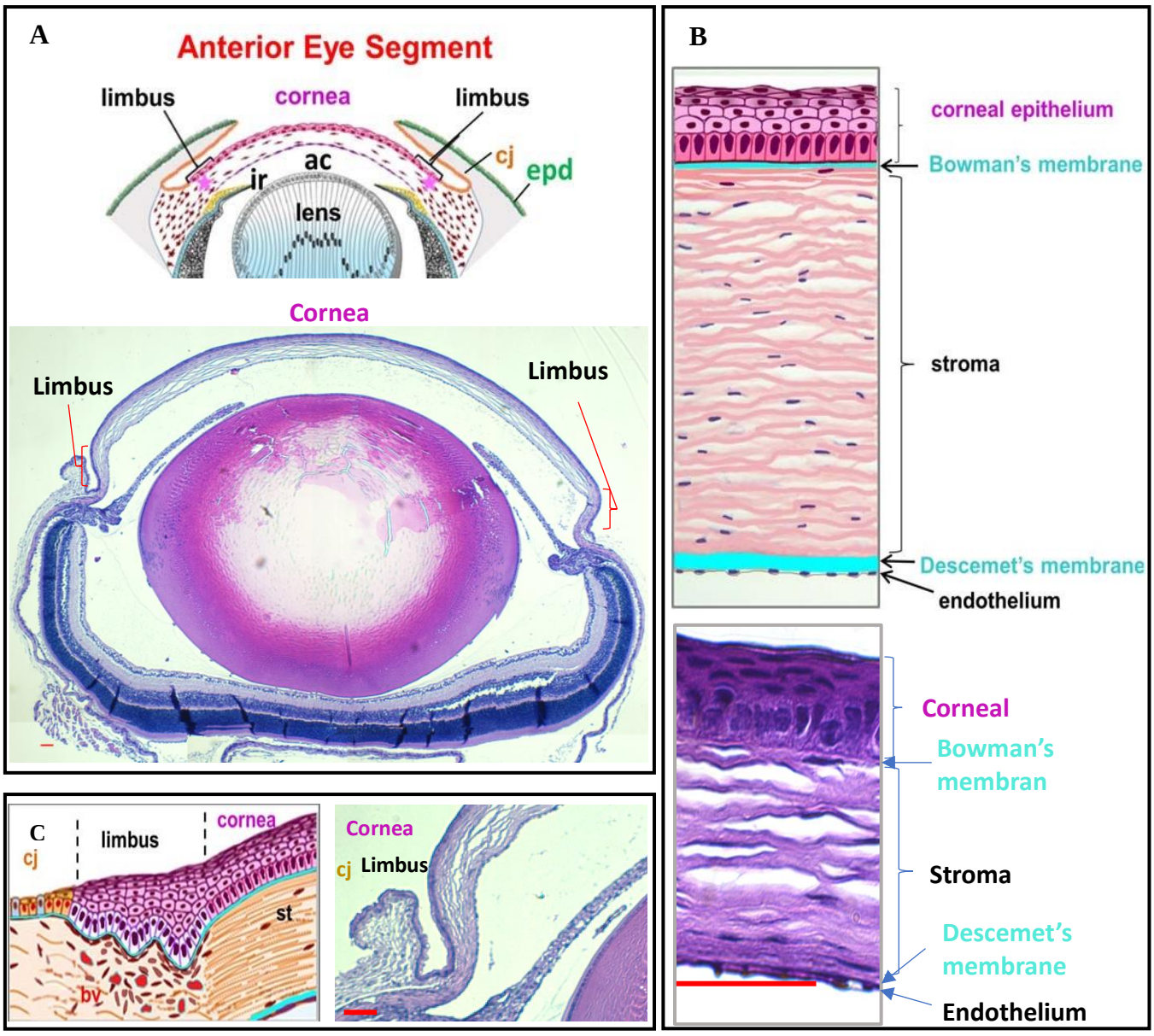

Figure 1: Structure of cornea. (**A):** Schematic representation of anterior segment of cornea showing different components of eyes; Lens, cornea, limbus, conjunctiva, retina. Photograph of immunofluorescent labelling of adult mouse anterior segment of whole eye. (**B):** Schematic representation of corneal structure with five different layers; corneal epithelium, Bowman's membrane, stroma, Descemet's membrane and endothelium. Photograph of immunofluorescent labelling of adult mouse central cornea. (**C):** Schematic representation of limbal structure showing thickening in cornea epithelium and presence of blood vessels (bv) in stroma. Photograph of immunofluorescent labelling of adult mouse limbus. Figure modified form Dhouailly et al., 2014.

2.2.2. Corneal organogenesis

Although the optical functions of lens and cornea are related to each other, in mammals their development processes are separate from each other. During early embryonic development in different stages, both the lens and cornea are derived from cranial ectoderm. (Figure 2). First, the neural crest is formed by invagination of neuroectoderm, then a bulge is seen which will become the optic cup. This optic cup spreads towards the interior part of the surface ectoderm, and the thickening of overlying cells of surface ectoderm forms the lens placode. Then, a cavity like structure is formed due to invagination of the lens placode which continuously invaginates until a hollow lens vesicle separates from the surface ectoderm (Collomb et al., 2013)(Greiling & Clark, 2008). At the same time of forming lens placode, a primitive epithelium is also forming side by side that is two cells in thickness and is contiguous with the surface ectoderm.

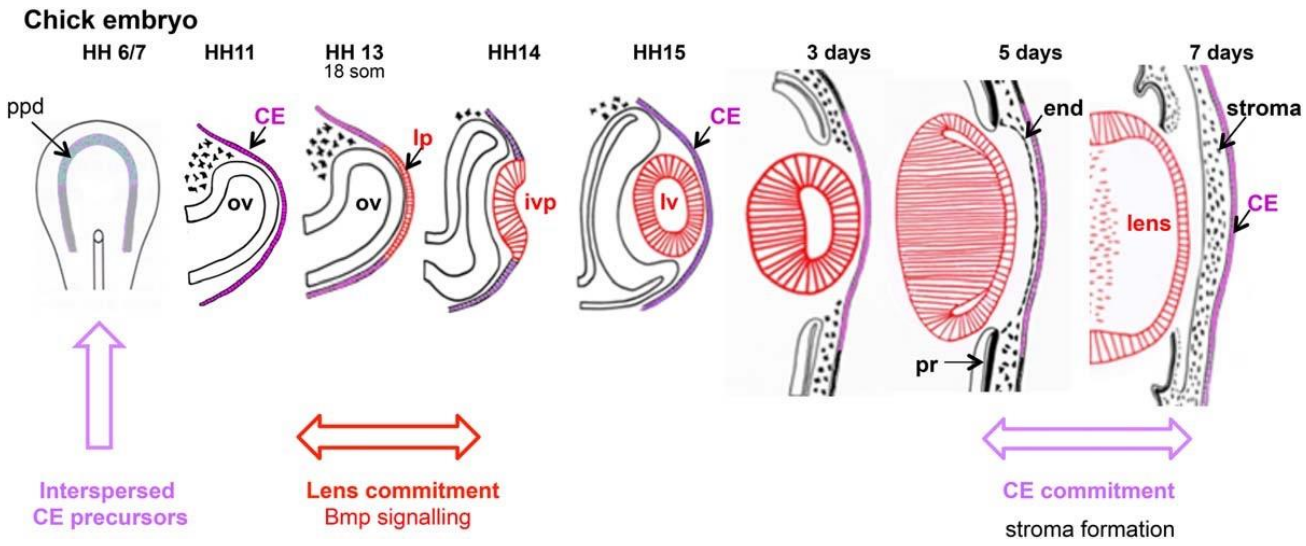

Figure 2: Illustration of formation of lens and cornea in chick embryo. At Hamburger and Hamilton (HH) stage 6/7 corneal ectoderm (CE) precursor is required at neural plate to form lens between HH stages 13-14 and then only cornea is committed between embryonic days E5-E7. end, endothelium; ivp, invaginating lens placode; le, lens; lv, lens vesicle; ncc, neural crest cells; nr, neural retina; oc, optic cup; ov, optic vesicle; lp, lens placode; ppd, preplacodal domain; pr, pigmented retina; st, stroma. Figure copied from Dhouailly et al., 2014.

In the human embryo, this process is apparent at about five weeks, and for next one to two weeks it stratifies to three to four cell layers thick. By that time, formed eyelids fuse to each other, and the process of lens forming completes and disconnects from the ectoderm. Corneal endothelium and the stromal keratocytes are formed by the migration of waves of neural crest cells into the space between the lens and epithelium almost immediately after the separation of the lens from the corneal epithelium. Migration of waves of the neural crest cells are species specific (Zieske, 2004). In rodents, cattle, rabbits and cats, it has been observed that there is only one migration of this wave of cells forming both endothelial cells and keratocytes, while in other species such as reptiles, birds, chicks, humans and other primates, two waves are seen first forming endothelial cells and then keratocytes (Cintron et al., 1983).

2.2.3. Corneal epithelium

Corneal epithelium is a very dynamic, stratified, non-keratinizing squamous layer tissue characterized by extreme uniformity from limbus to limbus. Corneal epithelial cells do not lose nucleus and undergo extensive keratinization unlike other epidermis. Corneal epithelium is 5-10 cell layered thick with three different types of cells. Basal cells are situated at the bottom of epithelium which are cuboidal to columnar shape, above basal layer there is suprabasal cell layers and superior to suprabasal cells, superficial cell layers are situated. During embryonic stages from E12.5 through E18 cornea starts to differentiate into two different layers, basal cell layer remains undifferentiated and expresses keratin 14 (*Krt14*) while suprabasal cell layer starts to differentiate by E14.5 thus expressing the cornea-specific epithelial differentiation marker *Krt12* (Tanifuji-Terai et al., 2006). *Krt12* and *Krt3* are present only in suprabasal limbal cell layers while basal cell layer expresses Krt5 and *Krt14* pair. In adult suprabasal layers the relative distribution of *Krt3* and *Krt12* varies from species to species. For example, in human and guinea pig *Krt12* were found more expressed in peripheral area than *Krt3* (Dhouailly et al., 2014). Within same corneal epithelium thickness varies such as thickness of a limbus varies from peripheral cornea and central cornea. Corneal epithelium thickness differs between species as well like mouse has thickest epithelium at central cornea while in peripheral cornea and limbus has few layers but in human limbal epithelium is the thickest with about 8 - 10 cell layers while central corneal epithelium has 5 – 6 cell layers (Z. Chen et al., 2004).

Cornea in rodents are only one or two cell layers thick until seven days of age (P7), but just prior to eyelids opening, which happens in twelve to fourteen days of age (P12 - P14), cornea undergoes for

massive development and differentiation (Chung et al., 1992). By the time of eyelids opening, the thickness of epithelium will be double the size (4 – 5 cell layers) compared to size at 1st week. Size of corneal epithelium continues to grow and by the 3rd week it will be 5 – 6 cells layered thick and by 4th week it reaches to adult stage that is 6 – 7 cells layered thick (Zieske, 2004).

During development of corneal epithelium, change in the fundamental shape of cells also happens along with change in numbers. Shape of basal cells are generally cuboidal to columnar after third week but before eyelid opening it shaped a rounded to cuboidal while before tenth day cells showed a flattened, ovoid shape (Chung et al., 1992). This change in shape of cells happens only in the central cornea not in limbus. Basal cells of the corneal epithelium start to co-express *Krt12* and *Krt14* only after 6 months of birth when corneal epithelium only starts to become fully differentiated. The rate of expression of *Krt12* in corneal epithelium in mouse and many basal epithelial cells of central cornea does not express *Krt12* remaining undifferentiated which shows that cornea epithelium are not fully matured until 7 months after birth (Tanifuji-Terai et al., 2006). During stratification, basal cell flattens, and forms intracellular junctions known as desmosomes as they leave the basal cell layer. In mature cornea, at least three to four layers of these flatten cells or wing cells are present. Superficial cell layers are formed as the basal cells stratify upwards and become flatten (Rheinwald & Green, 1975).

2.3. Limbus

Limbus is the transitional zone that connects the central cornea to the opaque conjunctiva and sclera. It also contains non-keratinizing multi layered stratified epithelium underlined with highly strong and vascularized stroma. Limbal epithelium contains melanocytes, Langerhans cells and a network of blood vessels. The conjunctiva attached to it consists of goblet cells whereas it lacks those kinds of cells. In human, limbal epithelium is organised in radial fibro-vascular elevations known as the palisades of Vogt but in mouse limbus they are absent, which alternate with epithelial rete ridges. Limbal basal epithelial cells are least differentiated in comparison to the central corneal epithelial cells. These undifferentiated cells are small in size and round in shape which contains less cytoplasm (H S Dua et al., 1994). Different types of keratins are present in limbal epithelial cells, among these keratins most of them are expressed in less differentiated cells. Although there have been yet no markers identified to label limbal epithelial stem cells (LESC), by the help of the differential expression pattern of keratins we can still differentiate the different types cell population within the corneal epithelium according to their level

of differentiation (Moll et al., 1982) . The 64 KD keratin *Krt3* and *Krt12* are expressed in the suprabasal layer of limbus and entire corneal epithelium as well but are not found in the basal layer of limbus which leads to the hypothesis that the limbal basal epithelium contains SCs which are least differentiated cells of the epithelium (Kurpakus et al., 1990; Schermer et al., 1986)

2.4. Corneal epithelium and stem cells

In a lifespan of an organism, the surface epithelia are renewed continuously. Approximately every single month human epidermis is exchanged, while it takes nearly about a year to renew the corneal epithelium. SCs and transient amplifying cells are only the proliferative cells in every normal tissues thus the corneal epithelium also rely on these SCs to be renewed (Pellegrini et al., 1999). Mann in 1944, disclosed indirect evidence of SCs existence in the limbus when he detected the migration of pigmented basal cells from the limbus towards the wounded central cornea in rabbits (Mann, 1944). In 1971, Davanger and Evensen detected that the cells of the corneal epithelium endure strongly manifested centripetal migration. In healed eccentric corneal epithelial defects, they observed that in highly pigmented eyes pigment in the epithelium migrated in lines from the limbus to the central cornea. Thus, proposed that the corneal epithelium get renewed from a pool of cells located at the limbus (Davanger & Evensen, 1971). Later in 1989, Cotsarelis et al were the first to report the existence of subpopulation of slow-cycling limbal epithelial basal cells located in the limbus of the murine cornea that retained tritiated thymidine label for long time periods (Cotsarelis et al., 1989). Lately many other studies in animals have questioned this fact that corneal epithelial stem cells (CESCs) solely reside in the limbal region of cornea, rather the central cornea also possess similar proliferative potential as limbal cells (Majo et al., 2008a).

2.5. Limbal epithelial stem cells and its niche

Stem cell niche (SCN) is very special microenvironment consisting of the other cellular and extra cellular components in the vicinity which regulates the self-renewal and fate decision of SCs. There are lot of studies that suggest that CESCs are located at stem cell niche within the corneal limbus. The limbal basal cells are relatively undifferentiating with compared to central corneal epithelium, this was shown by Schermer et al., in their study where they studied the expression of *Krt3* (a major differentiation product of the corneal epithelium). *Krt3* was expressed throughout the central corneal epithelium while it was not expressed in limbal basal cells (Schermer et al., 1986). In several studies it has been illustrated that in comparison to the central corneal epithelium limbal epithelial cells have a much higher

proliferative potential in vitro (Ebato et al., 1987, 1988; Lindberg et al., 1993; Wei et al., 1993). Buck in 1985 and Auran et al. in 1995, showed that centripetal migration of peripheral corneal cells takes place toward the central cornea (Auran et al., 1995; Buck, 1985) aiding the evidence for supporting the limbal location of CESCs. Similarly, in early 90s' studies it was shown that there are catastrophic effects on the integrity and wound healing capacity of central corneal epithelium if limbal basal cells are destructed (J. J. Chen & Tseng, 1991; J. J. Y. Chen & Tseng, 1990; Huang & Tseng, 1991). Damaged corneal epithelium was effectively repaired with restoration of the corneal transparency and sight by transplanted limbal epithelium while there were failures with conjunctival epithelium (Kenyon & Tseng, 1989; Lehrer et al., 1998; Tsai et al., 1990; Tseng & Tsai, 1991).

Several studies have illustrated that LESCs located at the basal cell layer of the limbus is responsible to maintain the corneal epithelium. In animal experiment, trauma induced displacement and migration of pigments from limbus to central cornea is seen (BUSCHKE, 1949; Mann, 1944). Similarly there are several studies using genetic fate mapping have also suggested the centripetal renewal of the corneal epithelium from limbus to the central cornea (Amitai-Lange et al., 2015; Collinson et al., 2002; N. Di Girolamo et al., 2015; Dorà et al., 2015). Thus, in order to maintain the homeostasis of corneal epithelium, LESCs need to divide asymmetrically maintaining the balance of self-renewal and replacement. Therefore, one of the daughter cells should remain within the SC pool while another migrates towards the central cornea as a differentiated transit amplifying cell (TAC). This TAC has high but limited proliferative activity that migrates upward from basal layer to the superficial layer. After reaching to the superficial layer, these cells after mitotic division becomes terminally differentiated cells (TDCs) which gets removed from the ocular surface (Figure 3) (Beebe & Masters, 1996).

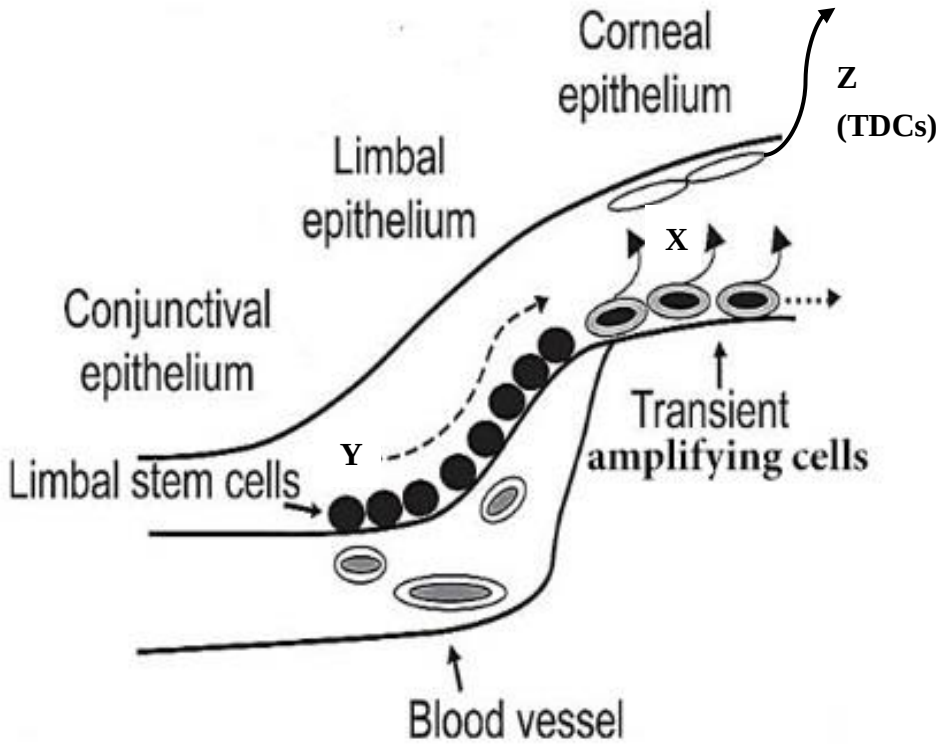

Figure 3: Corneal epithelial cell maintenance by LESC. Limbal stem cells located in the limbus generates TACs (X) which migrates centripetally (Y) to the central cornea which moves upward to superficial layer after a discrete number of cell divisions and then finally sloughed from the surface (Z). Figure modified from Kayama et al., 2007.

In Thoft and Friend's model, the epithelial cell mass is maintained by three independent phenomena in which X describes the proliferation of the basal epithelial cells, y is the centripetal movement of the limbal cells and Z is the cells, sloughed from the surface (Figure 3). Thus according to them rate at which corneal epithelium is self-renewed can be explained by the X, Y, Z hypothesis which predicts that the equation X + Y = Z represents the balance between cell proliferation and cell loss (Thoft et al., 1983).

Although till date, there is no single reliable LESC marker has been identified, few proteins appear to be stated in the limbal basal epithelial layer where LESCs are supposed to be situated. Expression of these proteins in those area possibly indicates that these proteins might be the putative LESC markers (Table 1).

Table 1: Expression of putative stem cell markers in central corneal epithelium and limbal epithelium.

	Central Cornea	Limbus	References
ABCG2	-	+ + +	(Z. Chen et al., 2004) (Budak et al., 2005)
p63	-	+ + +	(Pellegrini et al., 2001)
Bmi1	-	+	(Barbaro et al., 2007)
Frz7	-	+ + +	(Mei et al., 2014)
ABCB5	-	+ + +	(Ksander et al., 2014)
N-cadherin	-	+	(Higa et al., 2009)
Notch-1	-	+ +	(Thomas et al., 2007)
Cytokeratin 12	+ +	-	(W. Y. W. Chen et al., 1994)
Cytokeratin 14	+	+ + +	(Figueira et al., 2007)
Cytokeratin 15	-	+ + +	(Schermer et al., 1986) (Yoshida et al., 2006)
Cytokeratin 19	+	+ + +	(Z. Chen et al., 2004) (Yoshida et al., 2006)

+ + +: high expression, + +: moderate expression, +: weak expression, -: no expression

2.6. Bmi1

Bmi1 is a polycomb ring finger oncogene that plays important roles in cell cycle regulation, cell senescence, and cell immortalization. *Bmi1* has been reported as stem cell marker in number of organs where it is accountable for the maintenance of adult self-renewing haematopoietic cells and is vital for the maintenance of neural stem cells (distinguishing their self-renewal from progenitor cell proliferation) (Molofsky et al., 2003; Park et al., 2003). Defects in haematopoiesis, skeletal patterning and neurological development have been seen in *Bmi1-/-* mice (Park et al., 2003). It is believed that amplified proliferation of cells is promoted by *Bmi1* but maintenance of the stem cell phenotype is highly correlated with high expression of *Bmi1* (Umemoto et al., 2006). In human limbus, *Bmi1* expression was detected while in the central cornea it is expressed extremely low level (Barbaro et al., 2007; Umemoto et al., 2006). Expression of *Bmi1* was also seen in cells lining of bioengineered limbal crypts (*in vitro*) (Levis & Daniels, 2016) and also in holoclones isolated from the pig cornea (Majo et al., 2008a). Thus, *Bmi1* expression in cornea identification makes easier to study the maintenance of homeostasis and tissue renewal process of the corneal epithelium.

3. AIMS OF THE STUDY

In this project, I aimed to address the development of the corneal epithelium using mouse as a model organism. Specially, I am in the role of *Bmi1* in development process and tissue homeostasis of murine corneal epithelium. However, in this study, my aims were:

1. To study the chronology of maturation of mouse corneal epithelium. To do this I will be looking for expressing pattern of *Krt19* in different timepoint of animal's age.
2. To correlate the growth of eye size with proliferation of corneal epithelial cells.
3. To know the fate of *Bmi1+* cells and to investigate the involvement of these *Bmi1+* cell population in maturation and proliferation of corneal epithelium.
4. To validate these protein expressions of *Bmi1* via RNA level expression.

4. MATERIAL AND METHODS

4.1. Mouse lines

We used transgenic mice to conduct this study. For *Bmi1* lineage tracing/fate mapping, we took advantage previously reported mouse lines; $Bmi1^{CreER}$ and $R26R^{LacZ}$. $Bmi1^{CreER}$ and $R26R^{LacZ}$ were crossed with each other to create $Bmi1^{CreER/wt}$; $R26R^{LacZ/wt}$ animals. NMRI (wild type) mice were used for all other experiment performed in this study.

4.2. Genotyping by PCR

All the litters from *Bmi1-Cre* and *ROSA-LacZ* mice had to be genotyped to ensure that the sequences for *Cre* and *ROSA* were in the same individuals and to separate the double positive animals from other animals. The samples for genotyping were obtained from the tail or ear. These samples were lysed by using tail lysis buffer (Annex) with Proteinase K (Roche, USA) at +55º C for 2-3 hrs with the occasional vortex. The lysed samples were centrifuged (Eppendorf, Germany), the supernatant was collected, and the equal volume of isopropanol was added to precipitate DNA from the solution. Next, the mixture was centrifuged, the supernatant was discarded, and 70 % ethanol was added to the pellet. Again, the supernatant was removed after centrifugation and the pellet containing the DNA was dried in + 58º C. The purified DNA was dissolved in 1 X TE buffer (Annex) to protect the DNA from degradation. DNA was amplified with PCR (PTC-200 Peltier Thermal Cycler, Finnzymes, Finland). The mixtures and PCR programs, as well as the primer sequences, are detailed in Annex of this report. Finally, the amplified sequences were separated by agarose gel electrophoresis and visualized under ultraviolet light (UV) (Bio-Rad Laboratories, USA).

4.3. Tissue preparations

Whole head was dissected from the embryos and their lower jaw and brain was discarded. Only eyes were dissected from adult mice and for prenatal stages whole head samples were decalcified with 0.5 M EDTA (ethylene diamine tetraacetic acid) for two weeks. Those tissue samples were kept in Dulbecco's phosphate buffered saline solution to prevent them from drying. To preserve all possible morphological features and to prevent them from decaying, tissues were fixed in 4 % PFA overnight. Whole head tissues were decalcified in 0.5M EDTA pH 7.5 for about 8-14 days. EDTA was changed

every second day. Decalcified head samples and eye samples were processed through Leica ASP 300 automatic vacuum tissue processor to remove excess water from the samples and to infiltrate paraffin within the samples. Finally, samples were embedded in paraffin blocks (melted Histosec pastilles without DMSO, Merck, Germany). The microtome was used to make the sagittal section (5µm) and then baked on a +60º C heat plate to attach them on the adhesion slides. Some samples were stained with hematoxylin-eosin (Merck, Germany) (J.T.Baker, Holland) (Annex 1). The stained slides were mounted by Q path® coverquick2000 (VWR, USA). Remaining slides were stored in +4º C for other experiments like immunohistochemistry and immunofluorescence.

4.4. Immunohistochemistry

Paraffin sections were dewaxed with xylene series and decreasing alcohol series (100%, 94%, 75%, 50% ethanol and RO-water). After that the sections were washed with 1X PBS at room temperature. Antigen retrieval was carried out in the 10mM Na-citrate buffer, pH 6.0, at 121ºC in pressure cooker (Retriever 2100, Aptum Biologics) for 2hrs. After cooling down to room temperature, peroxidase blockage was done with 3% hydrogen peroxide (Sigma-Aldrich) in methanol (Sigma-Aldrich). Using permeabilization reagent (0.3% Triton-X in PBS) the sections were permeabilized, to prevent excess binding of the antibody to other proteins, then antibody blockage was performed by blocking solution (10% serum in 1% BSA (bovine serum albumin in PBS). Primary antibody for *Bmi1* expression *Bmi1* (Abcam, ab38295) in 1:200 concentration and for *Krt19* Keratin 19 (Abcam, ab52625) in 1:100 concentration were used and incubated for overnight at +4ºC, then, the sections were treated with anti-rabbit-horse radish peroxidase (ImmunoLogic) polymer at room temperature. Then sections were stained with DAB solution (Vector laboratories, USA). Sections were dehydrated in an ascending alcohol series (50%, 70%, 94% and 100% ethanol). After that they were counterstained with hematoxylin as explained.

4.5. Immunofluorescence

I did the deparaffinization as explained in the previous section. Dewaxed sections were blocked with 3% H_2O_2 in methanol in room temperature for 20 minutes and washed with 0.3%PBST for 10 mins. For antigen retrieval with heat induction, slides were place in 10Mm Na-citrate solution in milliQ water, pH 6.0, at 121ºC in pressure cooker for 2hrs and then I let the samples cool down to room temperature for 10 mins in Na-citrate buffer. Next the samples were washed with 0.3% PBST for 10 mins and blocked with 10% goat serum and 1% BSA in 0.3% PBST for 1 hour. After blocking samples were incubated

with primary antibody (Ki67; Abcam, ab16667) in 1:200 ratio with blocking solution at +4^{o}C for overnight. Next day, samples were washed 3 times with 0.3% PBST for 5 mins. Then samples were blocked with a Alexa 488 conjugated secondary antibody in 1:400 concentration. I also added Hoescht in 1:2000 for nuclear staining. Both substances were diluted in 5% BSA in 0.3% PBST for 2 hours at room temperature. Then samples were washed once with 0.3% PBST, 2 times with 0.1% PBST and 2 times with PBS for 5 mins each. Finally, samples were mounted with Vectashield (Vector Laboratories).

4.6. Eye size measurements and quantification of *Ki67+* corneal epithelial cells

Eye size was measured in two different groups; neonatal and postnatal mice. In neonatal, there were four different time points i.e., E13.5, E14.5, E16.5 and E18.5. Measurement of eyes for this group were done from processed eye tissue. Once the sections from these processed eyes were stained with hematoxylin and eosin (as explained above), they were photographed under microscope (Zeiss Imager) and measurement were done using ZEN software (blue edition, Carl Zeiss). Each time point had n=3 and most possible the biggest eye section was taken to measure. Then each section was measured form three different direction two as diagonally and one from top of the eye section to the bottom, then the average of these measurements were used as the actual measurement of neonatal samples. For postnatal mice I used four different time points i.e., P0, P7, P14 and P21. Measurements of eye size were done from fresh, enucleated eyes (n=3). After immunostaining, quantification of *Ki67+* cells were done manually by counting 20 serial sections of 5µm thickness from 3 different individuals. For neonatal mice *Ki67+* were counted from whole corneal epithelium while counting of *Ki67+* from the postnatal mice was done separately for each compartment (limbus, peripheral cornea and central cornea) of corneal epithelium. I divided the measured regions accordingly, limbal cornea 6.4% (2x), peripheral cornea 14.6% (2x) and central cornea 58%. After counting the *Ki67+* cells they were normalized to the area (A) of the respective compartment by using formula *Ki67+* cells/(Ax5x20).

4.7. Lineage tracing and X-Gal staining

The appearance of a vaginal plug was regarded as the start of embryonic development (E0) and the day of birth was taken as the first postnatal day (P0). Lineage tracing experiment was performed to know the origin and progeny of the *Bmi1+* cells.

Upon exposure to Tamoxifen (a synthetic estrogen), an inducible form of Cre, (CreER) fused with a modified estrogen receptor followed by releasing the CreERT2 fusion protein from cytoplasmic sequestration. This protein then translocated to the nucleus where it intervenes recombination which remove a “stop sequence”. This removal of ‘stop sequence’ allow expression of LacZ, this mechanism is only possible in double heterozygous (*Bmi1*CreER+; ROSALacZ+) mice. LacZ gene encodes the β-galactosidase enzyme that hydrolyses β-galactosides into monosaccharides. X-gal (5-bromo-4-chloro-3indolyl-beta-D-galactopyranoside) is one of the β-galactosides which is used in this staining protocol. X-gal is cleaved by β-galactosidase into galactose and 5-bromo-4-cloro-3-hydroxyindole, the later compound is then oxidized into 5,5 ¢ -dibromo-4,4 ¢ -dichloro-indigo, is a blue color product which represent LacZ activity in that cell/tissue of that double heterozygous (*Bmi1*CreER+; ROSALacZ+) mice.

To detect lacZ activity in my samples, I used Xgal staining. Head or eye tissues were fixed with 2% PFA and 0.2% glutaraldehyde (GA) in PBS for 30 mins in +4oC. After 30 mins, tissues were rinsed with PBS and washed 3 times with Xgal wash buffer for 30 mins each with gentle rocking. Washed tissues were left overnight in Xgal staining solution at room temperature so that tissues will be stained well. Next morning tissues were washed several times with PBS. Finally, tissues were post fixed with 4% PFA at +4oC for an hour and then washed several times with PBS before the tissues were being processed to prepare paraffin blocks. Then, tissues were processed in tissue processing machine (Leica ASP 300 automatic vacuum tissue processor). Later on, paraffin blocks were sectioned with microtome and sections were counter stained with Nuclear Fast red. LacZ activity can be visualized under microscope by the appearance of blue signal.

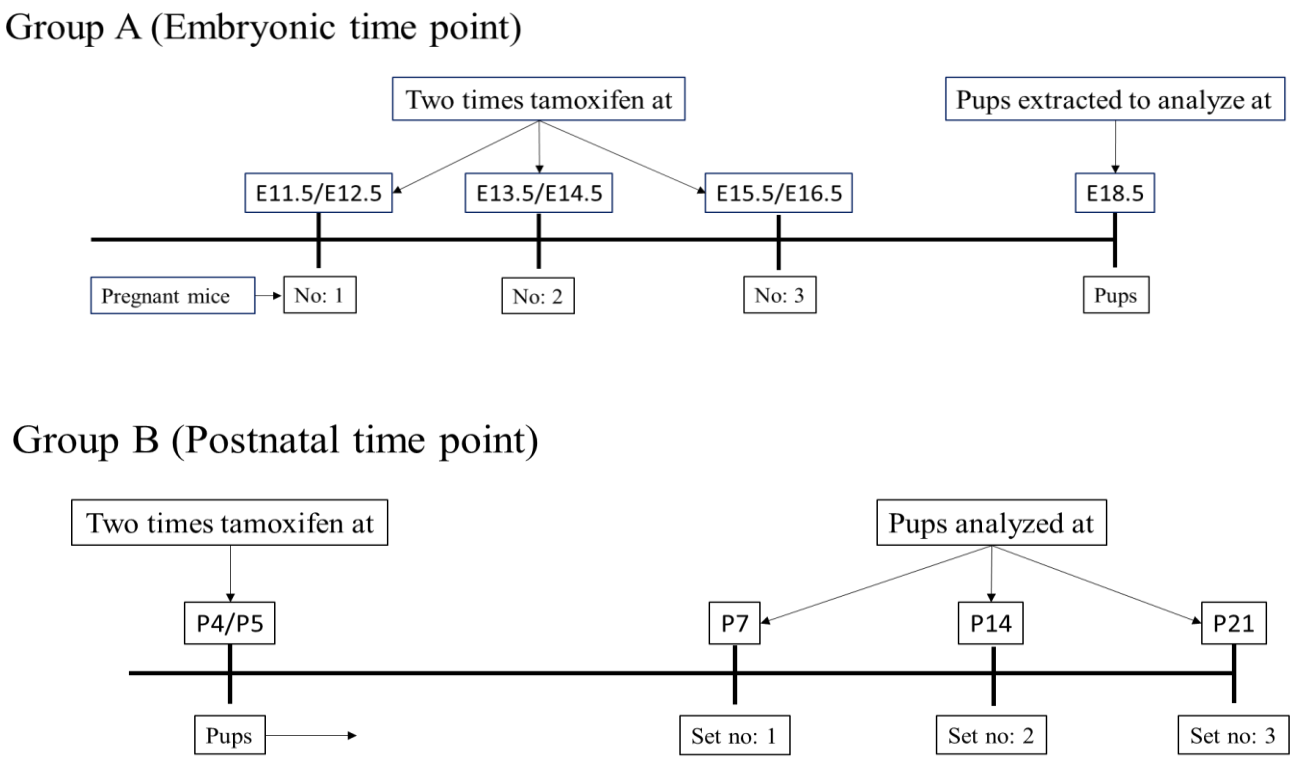

Figure 4:We followed two different experimental setups to study the origin and progeny of the Bmi1+ cells. Group A (Embryonic time point) consist three different pregnant mice (No: 1, No: 2, No: 3) who were injected with tamoxifen twice for induction at different time (E11.5 & E12.5 for No: 1; E13.5 & E14.5 for No: 2; E15.5 & E16.5 for No: 3) of their pregnancy and their embryos were analysed at E18.5. Group B (Postnatal time point) consist of three sets of pups (Set no: 1, Set no: 2, Set no:1) from three different pregnant mice. Then all these pups were injected tamoxifen twice for induction at P4 and P5 but they were analysed at different time points Set no: 1 was analysed at P7, Set no: 2 at P14 and Set no: 3 at P21.

For this experiment, mice were divided into two groups; Group A (Embryonic time point) and Group B (Post-natal time point). Three pregnant mice from group A were injected twice with i.p. 200 µl tamoxifen (50mg per ml to corn oil, Sigma) at three different time point; first at E11.5/E12.5, second at E13.5/E14.5 and third at E15.5/E16.5 and their pups were analysed at E18.5 (Figure 4). While for group B (postnatal time points), all the pups from three different litters were injected with tamoxifen twice at same time point P4/P5 but they were analysed at three different time points; first at P7, second at P14 and third at P21 (Figure 4). As a negative control, one of the mice which were not double heterozygous was analysed for every time point.

4.8. RNAscope

RNAscope is the newest method for *in situ* hybridization. The biggest advantage of this technique is to detect single mRNA transcripts as well as to amplify the specific signals of target but not of background signals. Thus, it is useful for labeling mRNA with high sensitivity and specificity.

In this study, this technique was used to detect mRNA transcripts of the *Bmi1* gene. I used the kit from ACDBio (Advanced Cell Diagnostics) to conduct the experiment. For this purpose, after deparaffination of sections (as described in previous methods), section slides were incubated with hydrogen peroxide for 10 mins in room temperature (RT). Then after washing, the section slides were submerged into boiling target retrieval reagent for 17 mins maintaining temperature at around 98 - 102oC by covering with aluminum foil. After a new wash with distilled water and then with 95% ethanol, sections were left to air dry completely at RT. Then, the section slides were placed in a humidity chamber and treated with protease for 20 mins. After washing with distilled water these sections were incubate with a few drops of *Bmi1* probes for 2 hrs. in the humidity chamber in the HybEZ oven. After washing with 1X washing buffer (Annex 1), hybridization of AMP 1 - 4 were done; 30 mins incubation with AMP 1, 15 mins with AMP 2, 30 mins with AMP 3, 15 mins with AMP 4 in oven in humidity chamber. Washing with wash buffer was done between each AMP steps. Then sections were incubated with AMP 5 in humidity chamber in oven for 15 mins. After washing with 1X washing buffer, it was again incubated with AMP 6 for 15 mins. Then, sections were washed twice with 1X washing buffer at RT and incubated with detecting signal (Fast red A and B in 1:60 ratio) for 20 mins at RT in humidity chamber. After washing with milliQ, sections were incubated in 50% hematoxylin for 2 min at RT and again washed with distilled water and again repeated with fresh water until clear. Then, sections were washed with ammonia water and again washed with distilled water. For dehydration, sections were baked in 60oC for 45 mins on a hot plate on a hand towel, under a plastic cover. Once the slides were cooled down to room temperature, they were mounted with VectaMount (Vectashield) mounting medium and left to dry overnight. Olympus AX70 microscope was used for taking the photograph of the sections.

5. RESULTS

5.1. *Krt19* is a reliable marker for the naive corneal territory

Expression pattern of *Krt19* was examined first to evaluate the chronological events during the maturation of the mouse cornea. For this, DAB immunohistochemistry was done with the anti-*KRT19* antibody. I studied the expression pattern of *Krt19* on mouse corneal epithelium from different stages of embryonic and young mice. *Krt19*+ cells were detected throughout the corneal epithelium from limbus to limbus and in conjunctiva leading to the inner layer of the eyelid. this is visualized in Figure 5 for the embryonic mice and at P0 (Figure 5). Already by P7, there were gaps in the presence of the *Krt19*+ cells on central cornea while in limbus every cell was still positive for *Krt19*. Once the corneal epithelium

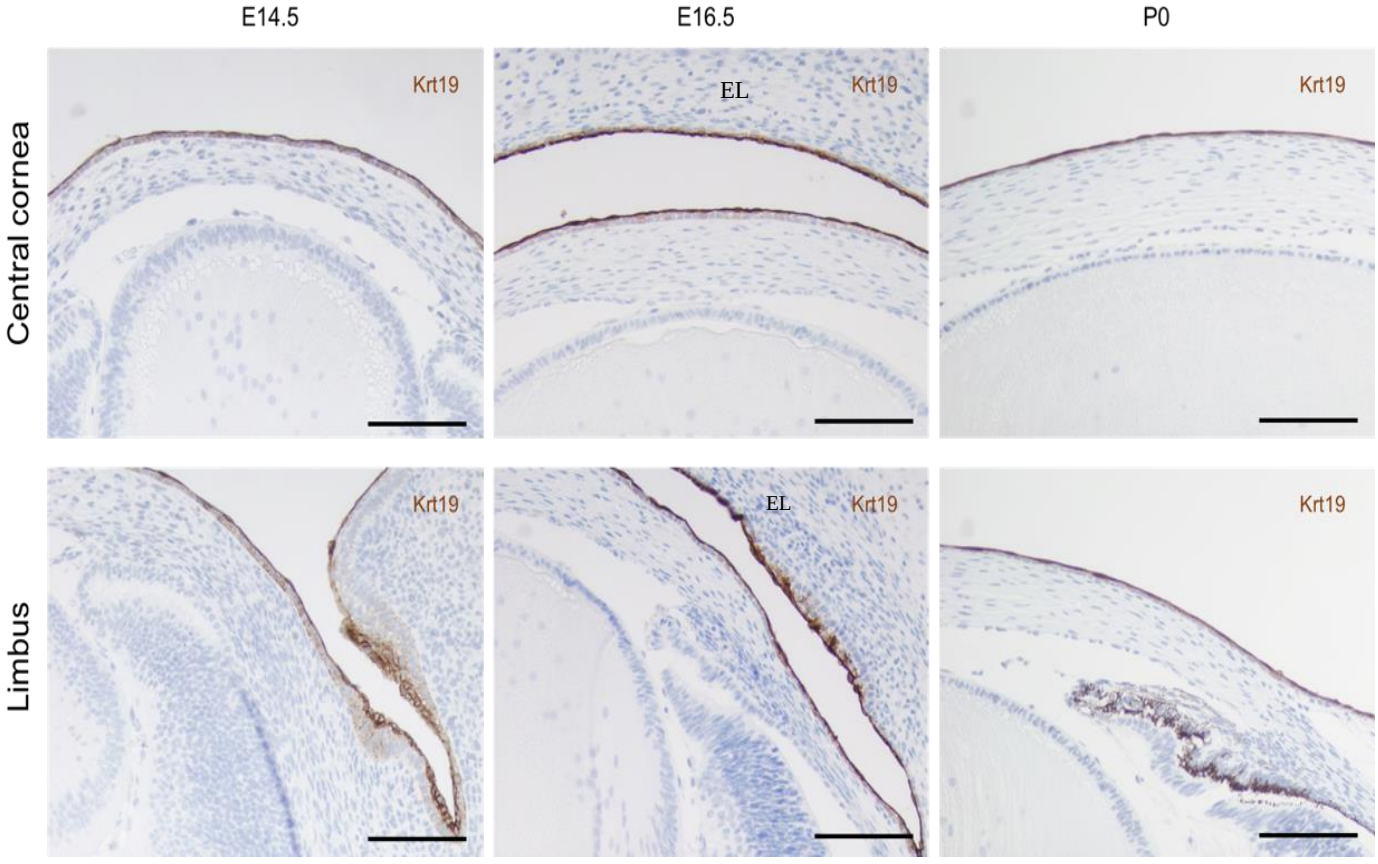

Figure 5. The expression of Krt19 in corneal epithelial cells at different time points until birth. Brown marker indicates the expression of *Krt19* expression. All the corneal epithelial cells from limbus to limbus are *Krt19* positive until birth. The expression of *Krt19* continue to the inner layer of the eyelid (EL) via conjunctiva. Scale bar is 100μm.

starts to stratify into multiple layers, there was a steady reduction in expression of *Krt19* in the central cornea and peripheral cornea. In the limbus *Krt19* was still strongly expressed. By P21 the expression of *Krt19* was lost from the central and peripheral cornea and it was solely expressed in the limbus (Figure 6).

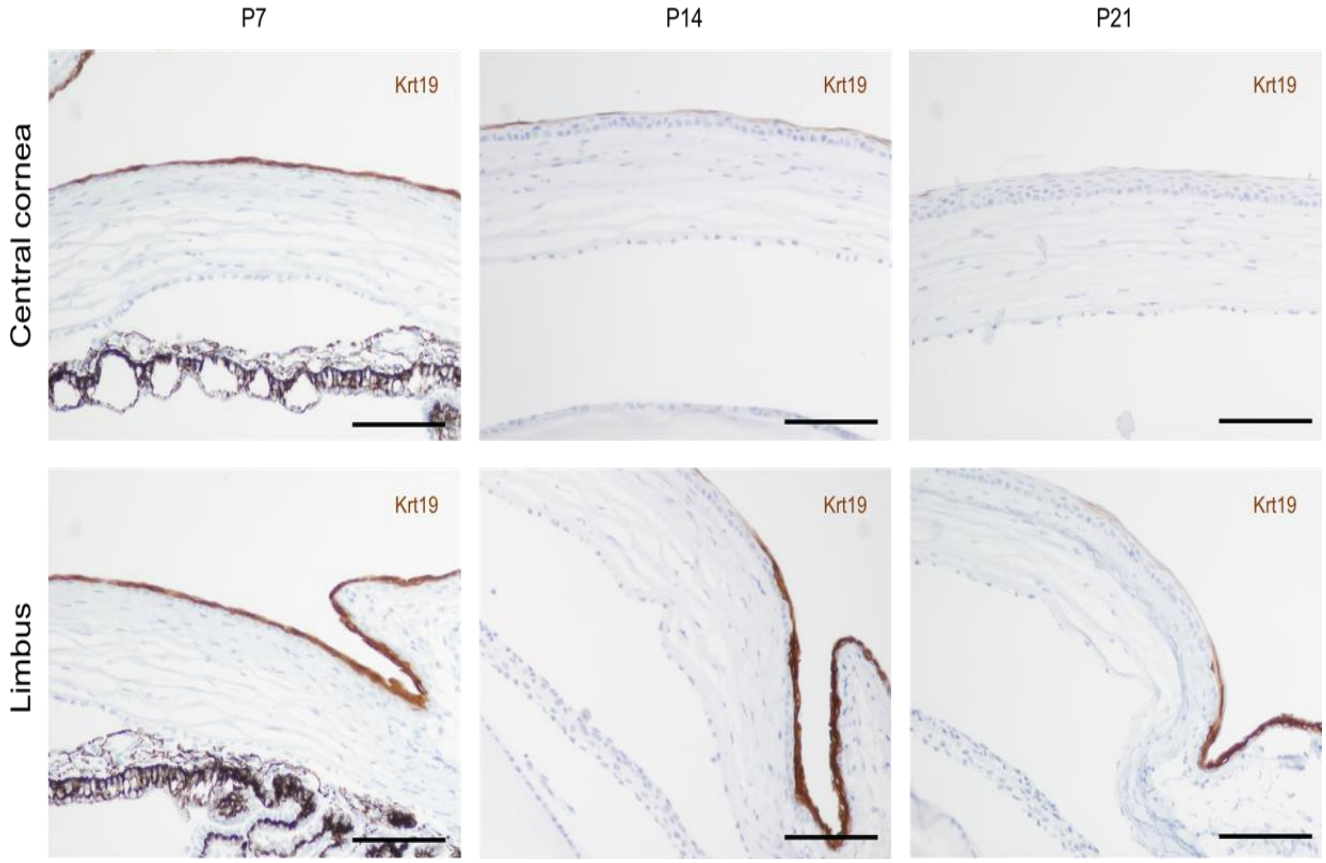

Figure 6: The expression of *Krt19*+ cells and its distribution on corneal epithelial cells at different time points after birth. Brown marker indicates the expression of *Krt19* expression. All the corneal epithelial cells from limbus to limbus are *Krt19* positive at P7. But already at P14 there were gaps in the expression of *Krt19* in central corneal epithelium. By P21, expression of *Krt19* was restricted to limbus. Scale bar is 100μm.

5.2. Growth and proliferation of the corneal epithelial cells of mouse eye

Here I have measured the diameter of eyes of different mice at different time points before and after birth. This was done in order to understand the correlation between the molecular maturation of cornea and the general eye growth. As shown in Figure 3, at prenatal stage from E13.5 to E18.5 the eyes grow significantly in great pace compared to the postnatal stages. From E18.5 to P0 we can see that there was increase in pace of growing eye but from P0 to P7 pace of growing eyeball increases and get the size of eye almost as one of adults (Figure 7). Eyeballs keeps on growing in steady speed until week 3 (i.e. P21) but then after there was no significant growth in eye size.

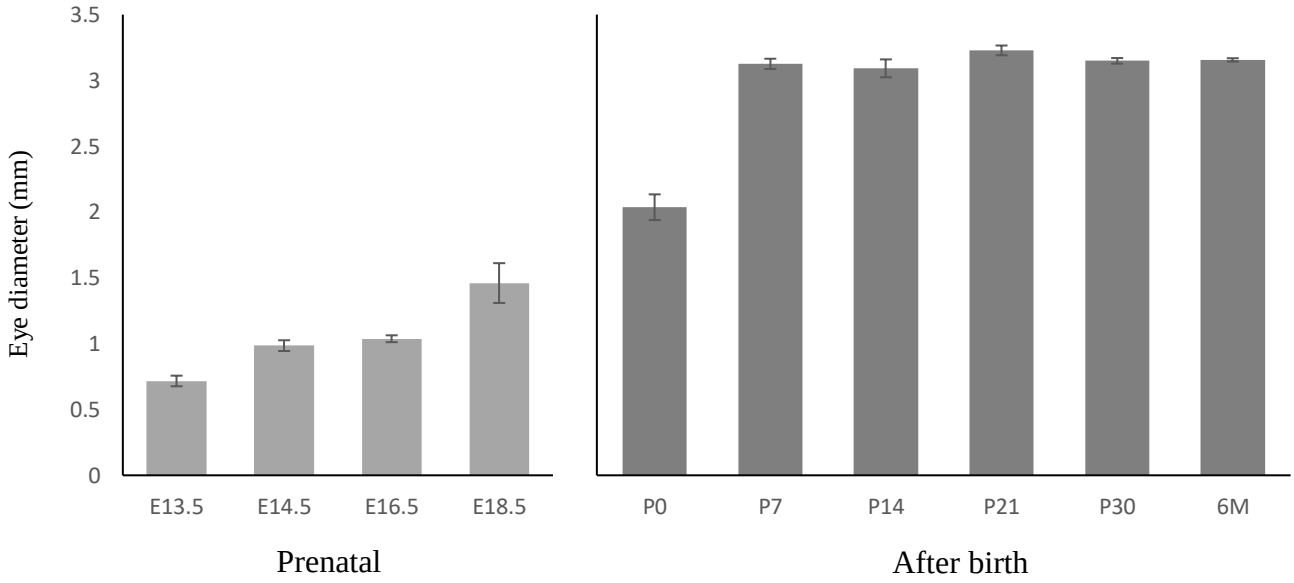

Figure 7: Growth of eye size with respect to the age. Graph shows growth of the eyeball is rapid before birth which continues till 1st week after birth. After there was a kind of halt in speed of growing of eye. Here measurement of eye for prenatal sample were done to processed tissues while for after birth sample whole fresh tissues were measured. Error bars, SEM.

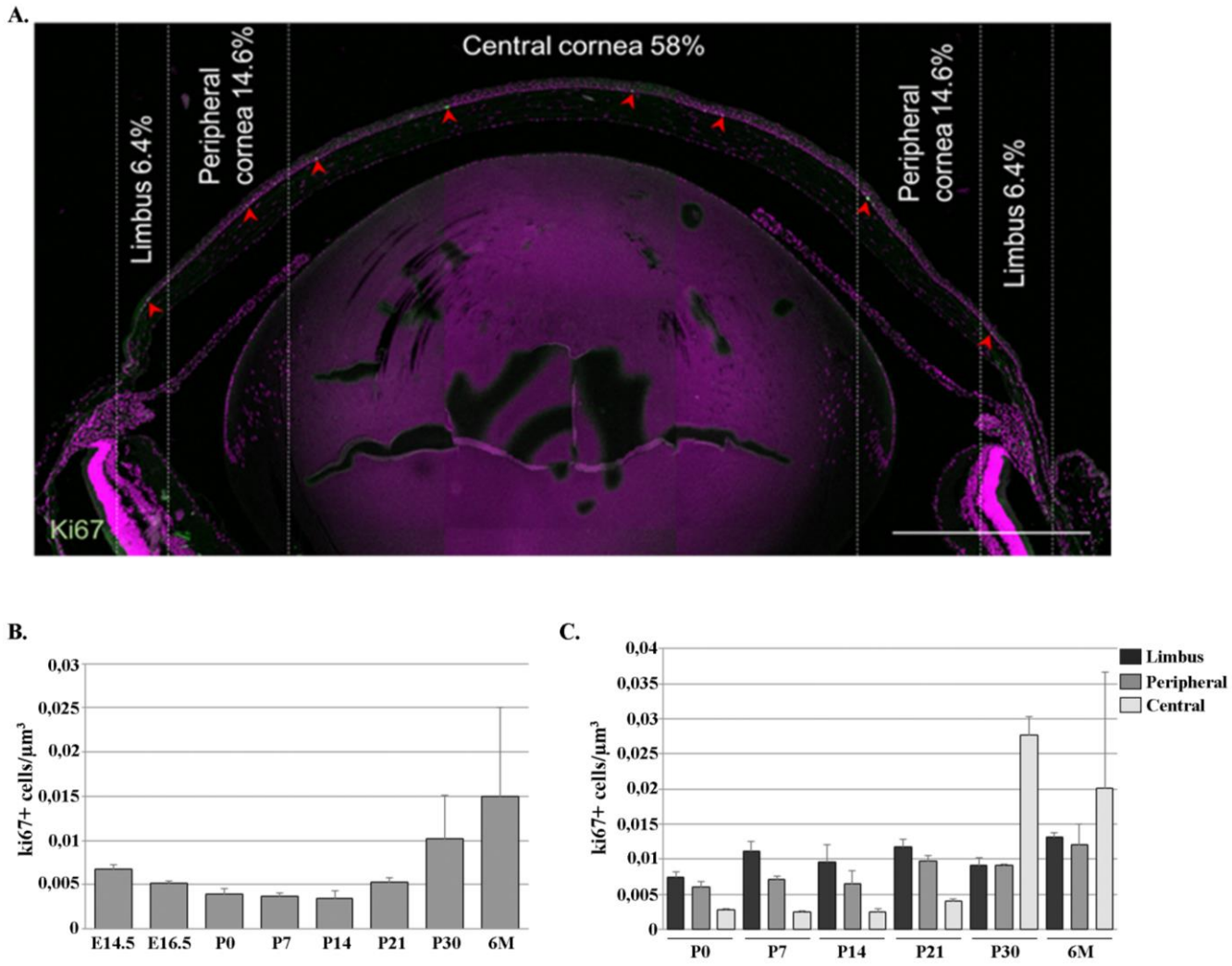

Figure 8: Quantitative analysis of the *Ki67*+ cells in the corneal epithelium at different ages. (**A):** The expression of *Ki67* and its distribution in the corneal epithelium at 2 weeks of age. *Ki67*+ cells are in green (pointed by red arrows). The corneal epithelium was divided to three different areas; for limbus: 6.4 % (2x), peripheral cornea: 14.6 % (2x) and central cornea: 58 % as shown. Hoechst (pink) for nuclear staining. Scale bar is 100µm. (**B):** *Ki67*+cells count per μm^3 is decreasing until P7. After the eyelid opening, there is a sudden increase in the amount of *Ki67*+ cells. (**C):** Proliferation at each corneal compartment. *Ki67*+ in the limbus are marked with grey, in the peripheral cornea with green and in the central cornea with red. The majority of the *Ki67*+ cells are located in the limbus from P0 until P21. After that the central cornea harbors the highest number of *Ki67*+ cells. Error bars, SEM.

Ki67 is the known marker for proliferation, thus here I have analyzed the expression of *Ki67* in mouse corneal epithelium and quantified the amount of *Ki67+* cells from E16.5 to 24 weeks of age. *Ki67* expression was detected in limbus, peripheral and central cornea of mice at all studied ages (Figure 8A). After quantifying the *Ki67+* cells, I saw that there was a gradual decrease in the quantity of the *Ki67+* cells until P14 from E14.5 (Figure 8B). To my surprise, there was a sudden increase of *Ki67+* cells after eyelid opening and epithelial stratification at P14. Until P21 limbus was more proliferative compared to the central and peripheral cornea, while after P21 the central cornea became more proliferative almost twice as that of limbus and peripheral cornea as shown in Figure 8C.

5.3. Localization of *Bmi1* expression in the murine corneal epithelium

Expression of *Bmi1*, p63 and Keratin 15 (*Krt15*) have been established as limbal markers in the adult human cornea by some the studies. Among these markers, *p63* and *Krt15* become remarkably limited to the human limbus previously before birth. Hence here I am interested in studying *Bmi1* expression, localization and their fate during cornea morphogenesis before and after the birth of mice.

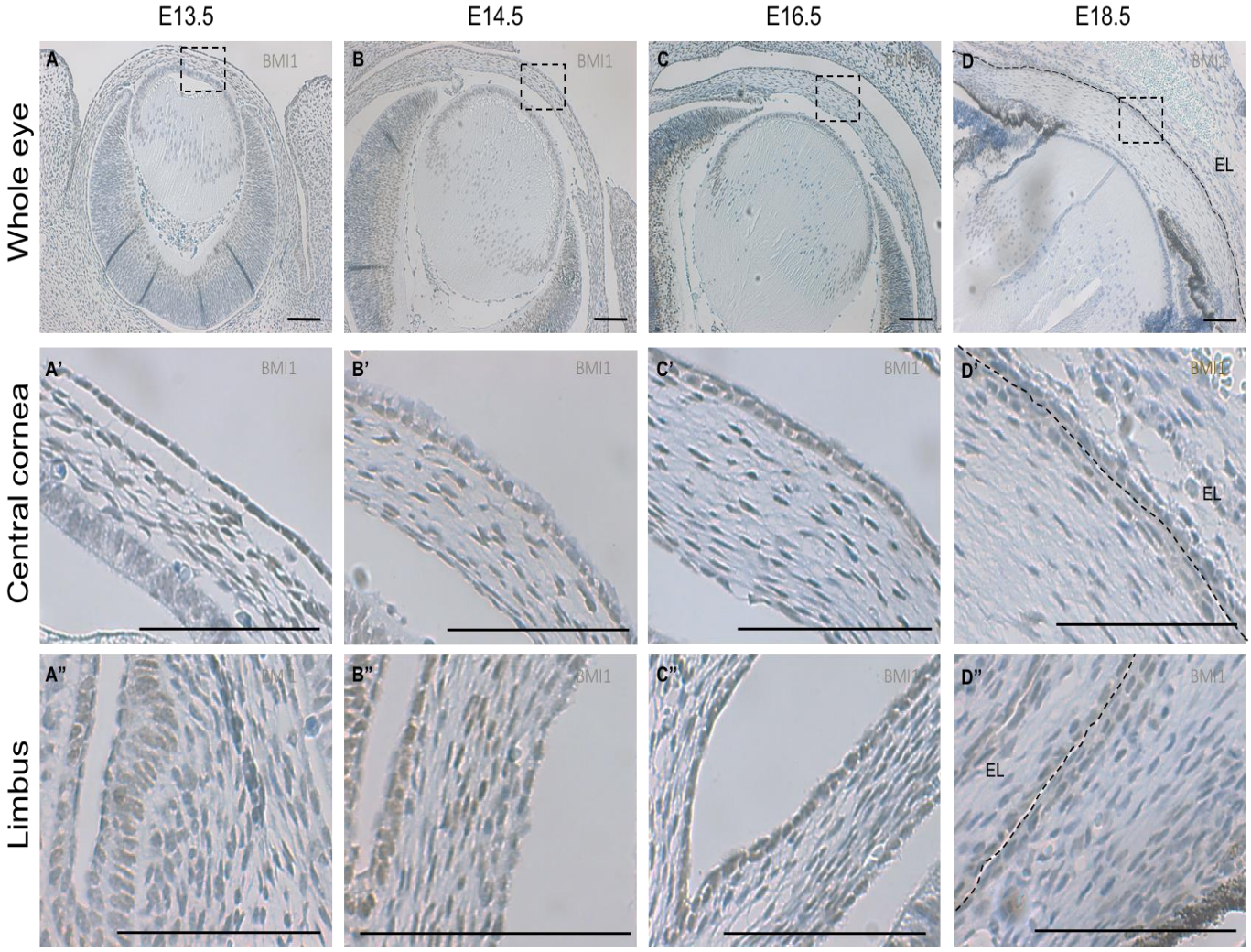

Figure 9: *Bmi1* is expressed throughout the corneal epithelium in prenatals. *Bmi1* immunostaining is brown. (**A-D'')**: Corneal epithelium is single layered, and every single cell expresses *Bmi1*. Black dotted line in **D-D''** separates eyelid (EL) and corneal epithelium. Scale bar is 100 μm.

Every single cell of corneal epithelium was *Bmi1*+ and the expression of *Bmi1* was seen very notably throughout the corneal epithelium from E13.5 until E18.5 (Figure 9).

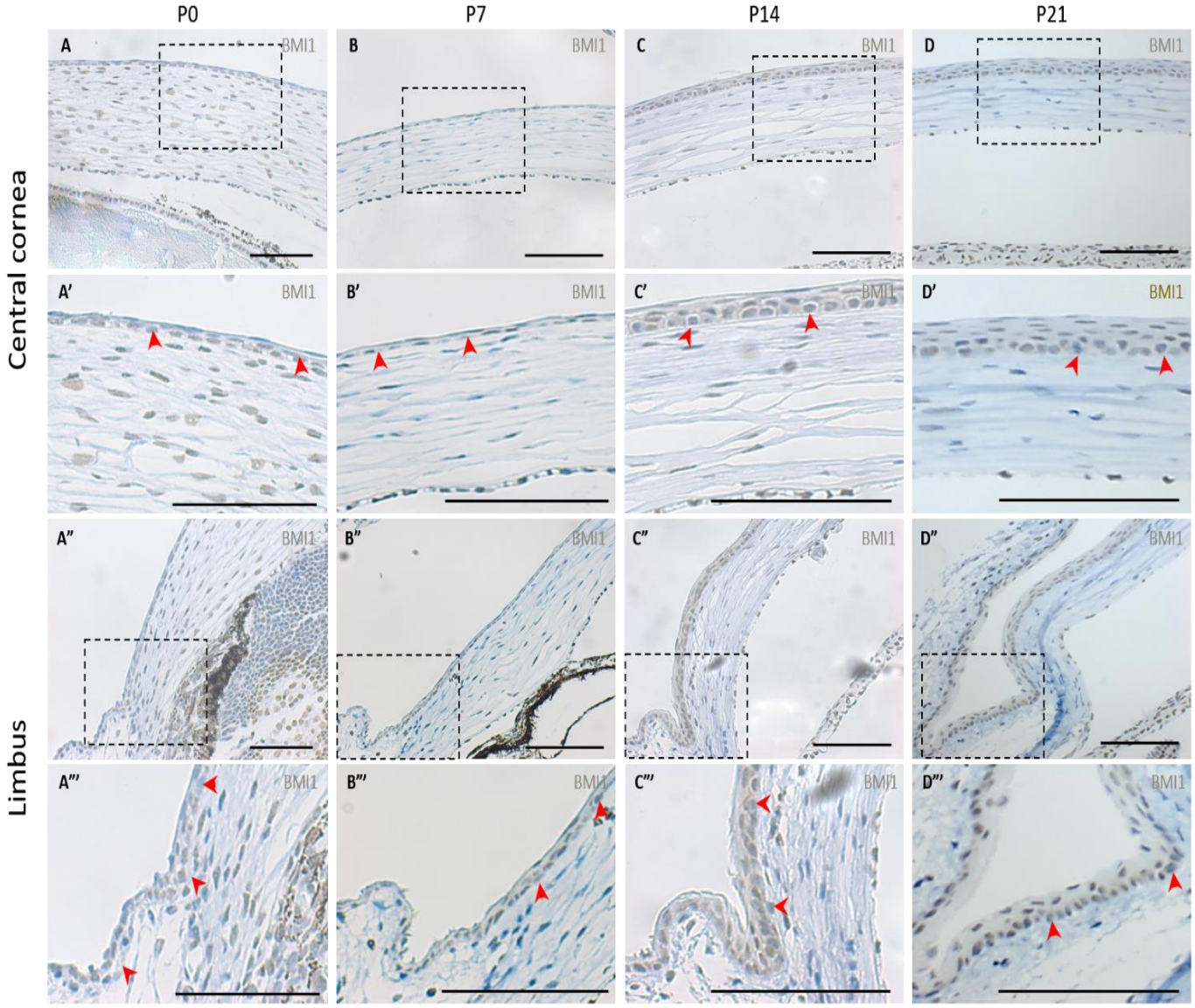

Figure 10: *Bmi1* expression is abundant in basal layer of corneal epithelium. *Bmi1* immunostaining is brown. Red arrowhead shows the cells with absence of Bmi1 expression (blue cells). After stratification (P14), we can see that maximum of *Bmi1*+ cells are present in basal layers and some are present in suprabasal. By the time of 3rd week (P21), we can see that most of the expression of *Bmi1*+ cells are located at limbus in comparison to central corneal epithelium. Scale bar is 100 μm

After the birth, from P0 we can see that there was presence some of cells on corneal epithelium which has no *Bmi1* expression. Before stratification, that is from P0 to P7 expression of *Bmi1* was present in basal and suprabasal epithelial layers and by the time of stratification (P14) and after that cells from

all layers expresses *Bmi1*. However, by P21 presence of *Bmi1*+ cells were considerably limited to the basal epithelium layer (Figure 10).

5.4. RNAscopes

Although there was not much difference in expression of *Bmi1*+ cells from E14.5 to P0, here I have investigated the level of RNA just to confirm that protein expression is the true expression for *Bmi1*+ cells. To investigate expression of RNA highly sensitive RNA in-situ hybridization technique was used. RNA expression pattern was exactly like protein expression on both E14.5 and P0. All the basal layer

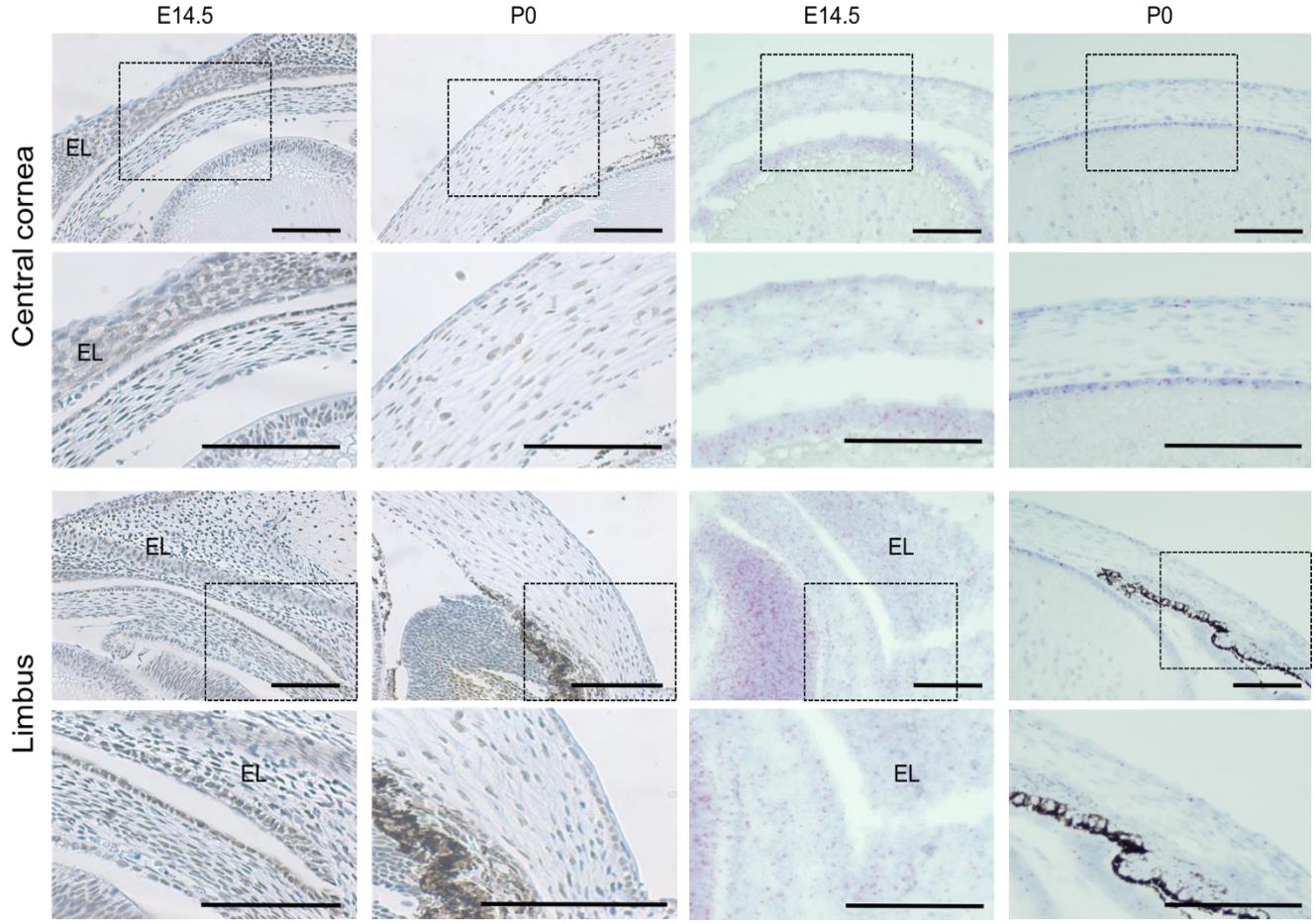

Figure 11: *Bmi1* expression level for protein and RNA are alike. *Bmi1* protein immunostaining is brown and *Bmi1* RNA level was detected by using RNAscope technique (In-situ hybridization technique) in pink color. For prenatal, all the cells express *Bmi1* in protein level and in RNA level as well whereas in neonatal there were presence of some negatively expressed cells for *Bmi1* in both protein and RNA level. Scale bar is 100 μm.

showed *Bmi1* RNA, which was like protein expression pattern for E14.5 while at P0 few *Bmi1* negative cells were present on both limbus and central cornea (Figure 11).

5.5. Genetic Fate Mapping of *Bmi1+* cells

Here we tend to investigate the involvement of *Bmi1+* cells in cornea renewal. For this we used offspring of $Bmi1^{CreERT/wt}$; $R26R^{LacZ/wt}$ mouse model and studied the progeny of labelled cells that were induced by using tamoxifen at different stages of age of animals. Labelled cells were induced by tamoxifen in three different pre-natal animals in different age but were all studied in same age within 2-7 days (Figure 12A). After performing histological analysis of these pre-natal animals, we hardly observed any *Bmi1+* cells (Figure 12B).

Similar experiments were performed in post-natal, where tamoxifen was injected in same age for all three different animals but then they were analysed in different age of time (Figure 13A). As similar to the results of pre-natal animal experiment I did not observed any *Bmi1+* cells after 1st week of induction. Then, as we follow for longer lime of intervals of 2-3 weeks *Bmi1+* clones were observed growing and expanding centripetally from the basal layer (Figure 13B)

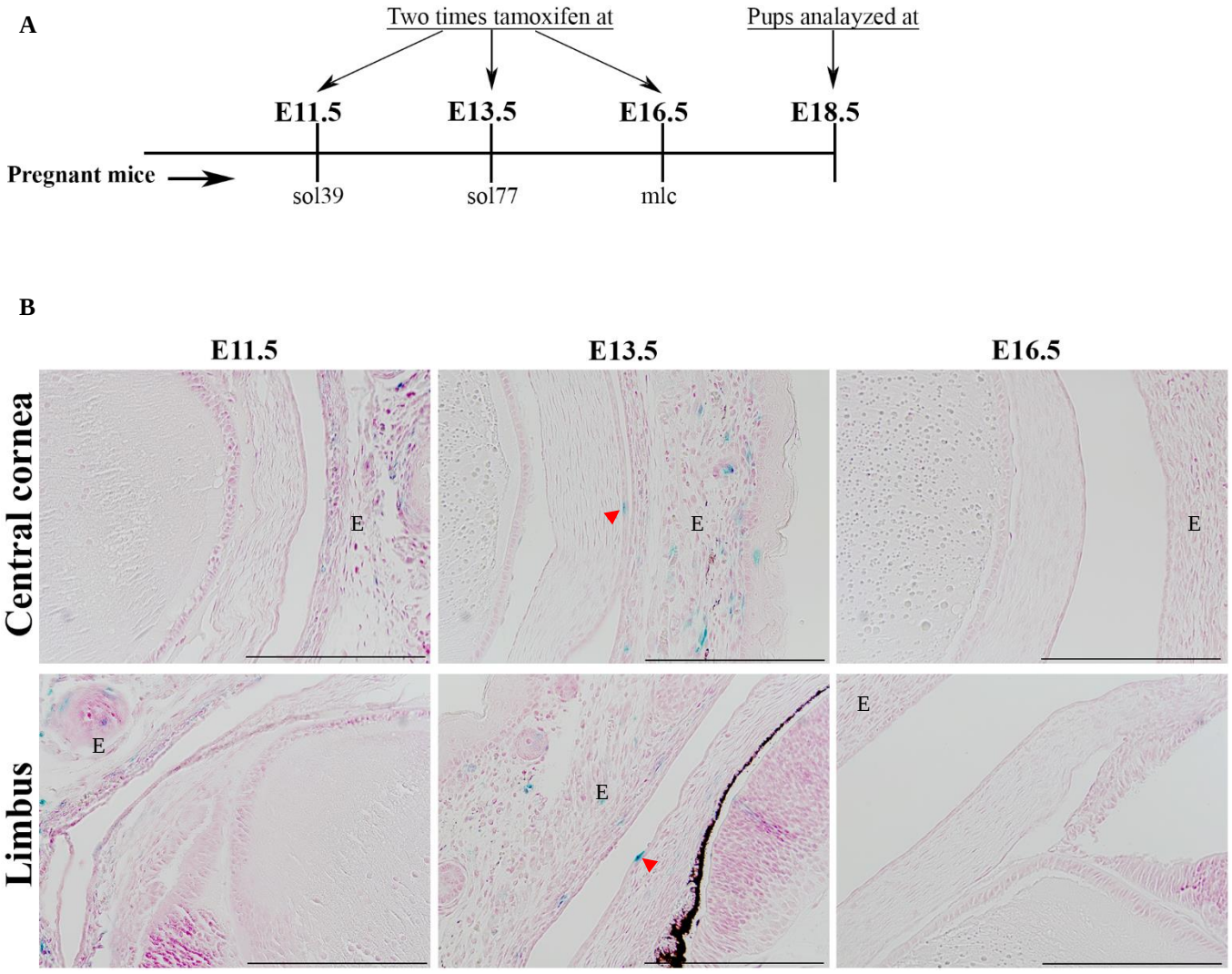

Figure 12: Genetic fate mapping of *Bmi1+* cells in pre-natal/embryonic stages. (A): Schematic drawing of the genetic fate mapping experiment performed in embryonic stages. **(B):** The histological sections of eye stained with X-gal staining. *Bmi1+* cells are indicated by red arrowhead. Scale bars are 100 µm.

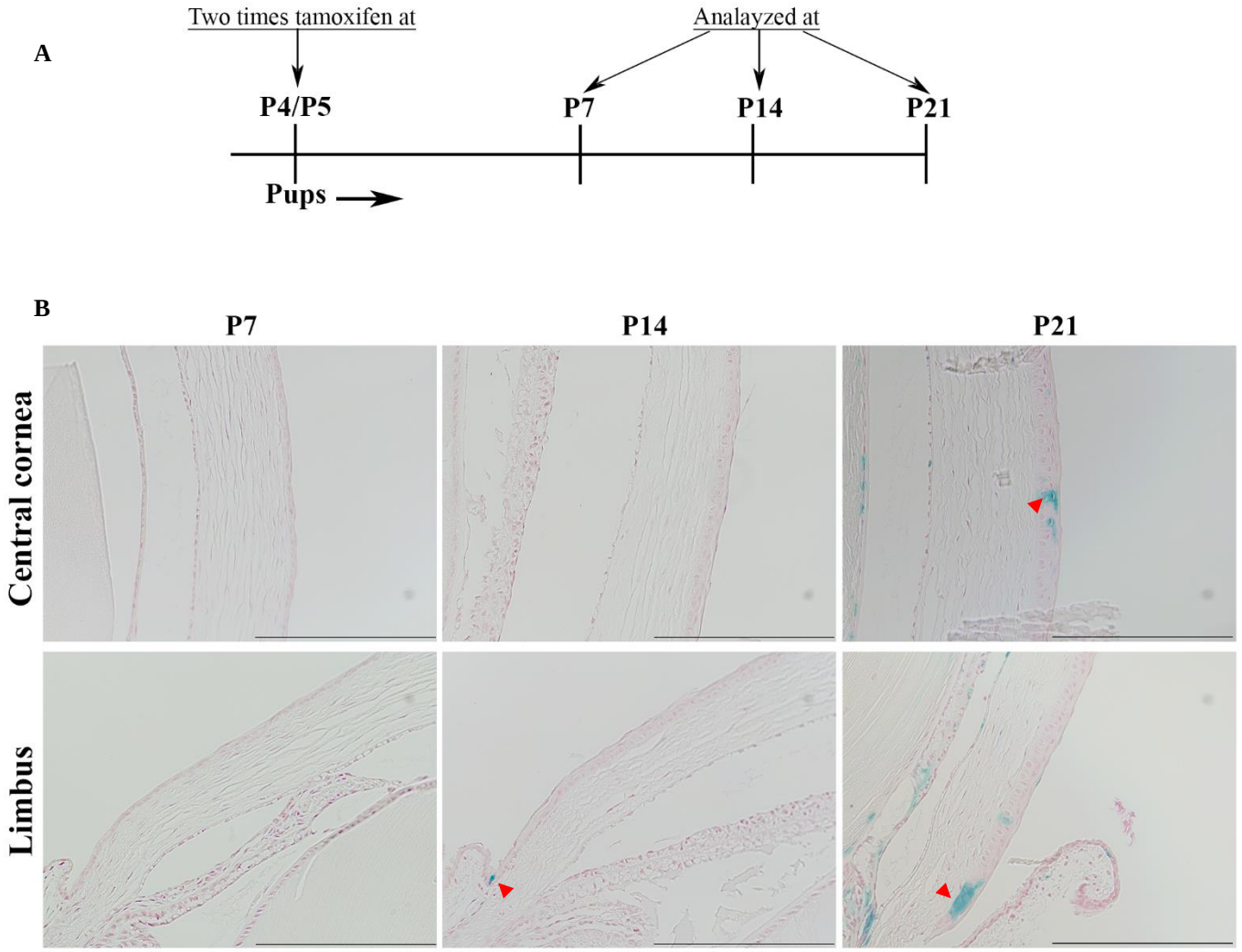

Figure 13: Genetic fate mapping of *Bmi1*+ cells in post-natal stages. (A): Schematic drawing of the genetic fate mapping experiment performed in embryonic stages. **(B):** The histological sections of eye stained with X-gal staining. *Bmi1*+ cells and their progeny in the central, peripheral and limbal cornea indicated by red arrowhead. Scale bars are 100 µm.

6. DISCUSSION

Isolation of mouse embryonic stem cells in early 80's brought whole new revolution in study of stem cell. In every living organism, tissue homeostasis is maintained by stem cells which resides in the specific regulatory microenvironment, known as SCN. Similarly, each and every epithelia are maintained by the stem cells residing within it, as cornea of the eye. To study epithelial stem cells, mouse cornea is an excellent platform. Many scientific groups have proved that limbus possesses the corneal stem cells which are responsible for renewable of corneal epithelium (Amitai-Lange et al., 2015; Collinson et al., 2002; N. Di Girolamo et al., 2015; Dorà et al., 2015). Although until the age of 5 weeks corneal epithelium is renewed locally and after that age limbal stem cells are activated for renewal purpose (Collinson et al., 2002; Dorà et al., 2015). This study is solely focused on the corneal maturation and involvement of *Bmi1* expressing cells which are the progenitor cells of corneal epithelium.

Cytokeratins are cytoskeletal proteins, that are expressed in during epithelial development and differentiation in distinct pattern. *Krt3* and *Krt12* are known as markers of corneal epithelial differentiating cells (M Kasper et al., 1988; Liu et al., 1993; Rodrigues et al., 1987). *Krt14+* cells were found in the basal and suprabasal layers of the limbal epithelium while there were no expression in the central epithelium (Wang et al., 2003). Similarly, few studies have shown that *Krt19+* cells localized in basal cells of the human and murine limbal epithelium (M Kasper et al., 1988; Michael Kasper, 1992; Lauweryns et al., 1993). However, in our study I found that the localization of *Krt19+* cells were on the superficial cell layer of the limbus (Fig 1 and Fig 2) which suggest that already during maturation of the murine cornea the limbal SCN is established. Therefore, I proposed that the superficial layer cells expressing *Krt19* is necessary for the maintenance of the stem cell niche. Thus, our results suggest that already before or by the age of 4 weeks, the renewal of epithelium that are originating from the limbus could start.

There are few studies conducted on a timeline for maturation of cornea at molecular level on murine cornea. A study showed that in the epithelium of central cornea of murine, the expression *Krt12* were observed in the mature and differentiating corneal epithelial cells only after the age of 12 weeks (Eghtedari et al., 2016). Apart from the result of this study (Eghtedari et al., 2016), there is another study which showed much shorter timeline for maturation of cornea. This study, studied the distribution of α9β1 integrin within the limbus of the mouse ocular surface where they found that at the age of 1 week

entire ocular surface contains cells positive for α9 integrin and already by the age of 2 weeks localization of α9 integrin begins to become regionally restricted (Pajoohesh-Ganji et al., 2004). In our study I used *Krt19* to study the chronology of limbal stem cell niche establishment where I observed that by the age of 3 weeks the limbal territory of corneal epithelium is already marked. Interestingly our results also correlate exactly to the expression pattern of α9β1 integrin+ domain. As similar to Pajoohesh-Ganji et al. study, in our study I detected *Krt19*+ cells throughout the corneal epithelium before birth and until at 1 week of age after birth entire corneal epithelium were expressed with *Krt19*, but the postnatal expression form altered gradually. At the age of 1st week, when corneal epithelium starts to stratify, expression of *Krt19* gradually decrease from the central and peripheral cornea which is followed at 2nd week of age. And by the time of 3rd week after birth the central cornea was stained totally negative for *Krt19*, but the protein was observed in the limbal region (Fig 1 and Fig 2). The expression pattern of *Krt19* is much shorter than that of *Krt12* because the cell population labelled by the *Krt19* mature more faster than that of *Krt12*.

During our study I observed the eyelids of the mouse are closed during the time of birth and only after two weeks (P14) of birth eyelid starts to open up, this finding is alike to several other studies (Zieske, 2004). Parallel to other studies, our study also showed the stratification of murine cornea is completed by postnatal day 21 (P21) (Zieske, 2004). In our study I found that steady growth of eye size of the mouse which has been correlated with the expression level of *Ki67*+ cells during maturation of mouse eye at all ages. A study confirmed that in dry eyes *Ki67*+ cells were present in suprabasal areas as results of apical cell surface damage to stimulate cells to cycle and proliferate through the entire epithelium (Fabiani et al., 2009). Same study showed that *Ki67*+ cells were detected in basal cell layer in normal eyes (Fabiani et al., 2009) which correlates to the result of this study, this suggests that basal layer in normal cornea basal layer of epithelium is responsible for epithelial cell proliferation and maturation of corneal epithelium. During gestational maturation, proliferating cells move from central cornea to limbus in human cornea (Pispa et al., 2008) while this case was not seen in distribution of *Ki67*+ cells in maturation of cornea in mouse in our study.

Over the decades there has been great advancement in technology and methods to understand biology and mechanism of limbal stem cell, yet science has not progressed to identify dependable markers that can differentiate stem cells from the early TACs. Due to which it is still unclear and controversial about the exact location of the human LESC niche (Harminder S. Dua et al., 2005;

Shanmuganathan et al., 2007; Shortt et al., 2007). Few study proposed p63, a nuclear transcription factor, as a possible stem cell marker of limbal stem cells (Pellegrini et al., 2001) but within second year of this claim, this was disproven by other study (Harminder S. Dua et al., 2003). Thus, till this date *Krt14* is only the known marker that has been used for genetic fate mapping of a restricted corneal cell population (Amitai-Lange et al., 2015; N. Di Girolamo et al., 2015). In this study, I focused on the corneal maturation and renewal pattern before and after birth, and genetic fate mapping is a powerful tool to study tissue renewal. For this purpose I studied *Bmi1*, a member of the polycomb repressive complex 1 which the most promising limbal stem cell marker in human that are localized in basal cell layer of limbus (Barbaro et al., 2007). First, I studied the expression patter and localization of *Bmi1* in the corneal epithelium before and after the birth of mice. In our result I observed that *Bmi1+* cells were mostly in passive state but somehow after the time of eyelids opening which 2nd week after birth, *Bmi1+* cells were active and expressed more vigorously than before. This effect might have happened because of damaged due to UV rays or any other physical/chemical means on cornea once it is out in open after eyelid opening process which suggests that *Bmi1+* cells might have some damage repairment capacity. I also observed the before birth where epithelium is mostly single layered, every single cell was expressing positive for *Bmi1*. While after birth, when epithelium start to stratify, I found *Bmi1* negative cells, more in central cornea in comparison to limbus (Fig 6 and Fig 7). To validate these results, I conducted experiment known as RNAscopes (In Situ Hybridization Kits, Hybridization Assays | Manual Assays, acdbio.com), to investigate RNA level of expression of *Bmi1* in corneal epithelium which also showed similar pattern of expression *Bmi1* RNA in central cornea and limbus (Fig 8). This result is little bit contrasting to other studies where *Bmi1+* cells were localized only in limbus (Barbaro et al., 2007; Sartaj et al., 2017). And for our genetic fate mapping and label retaining experiments I used two different genetically modified mouse model *Bmi1*CreERT/wt; R26RLacZ/wt and studied the progeny after cross mating. In this experiment I observed that *Bmi1+* cells cluster seen in the cornea specially in the limbal region which was spreading from the basal cell layer to suprabasal and then to superficial layer (Fig 8 and Fig 9). However, X-gal staining does not work homogeneously throughout the cornea, possibly attributable to low recombination homogeneous efficiency and stochastic silencing due to variegation of transgene expression (Dobie et al., 1997). I also observed that corneal epithelium is renewed locally by *Bmi1+* cells in provisional way. I observed that irrespective of the age of the animal, the murine corneal epithelium is locally renewed by *Bmi1* expressing progenitor cells. Thus, I concluded that *Bmi1+* sub-population cells are progenitor cells which get replaced by the limbal renewal. But for further verification, I need to

follow more age groups of the animal so that I can say that this result is repeated in older aged animals not only in young infants.

7. CONCLUSION

Our experiment suggests that the proliferating cells reside in the basal layer of cornea and the infant mouse cornea contains immature cells. Our experiment also advises that the maturation of mouse cornea is completed by the age of 2nd week at this timepoint eyelids of the mouse also open. Thus, our results conclude that these immature cells found throughout the infant mouse cornea will finally end-up locating at the limbus by final stage of corneal maturation. Our finding suggests that the *Bmi1+* cells are expressed all over the basal layer of cornea which locally renews the corneal epithelium concluding *Bmi1+* cells are the progenitor cells. Due one of our observation that expression of *Bmi1+* cells were more after eyelids opening time, it would be great to conduct experiment to study the effect of *Bmi1* cells on damaged cornea. I believe that detail study of genetic fate mapping of *Bmi1+* cells should be done by including more older age mice and follow the pattern of expression of *Bmi1* to know the actual fate of these cells. For future aspect I can study the colocalization of *Krt19* or *Ki67* and *Bmi1* expression in order to learn the relation between the expression of *Bmi1* and proliferation and maturation of corneal epithelium. Studying *Bmi1* KO genotype mice can open up paths to acquire knowledge about the effect of *Bmi1* in maturation of corneal epithelium and its phenotype. Similarly, further analysis of *Bmi1* positive and negative cells can convey light on the dynamic progression of epithelial renewal in the cornea.

8. ACKNOWLEDGEMENTS

This thesis work was carried out in Frederic Michon's research group in the Developmental Biology, Institute of Biotechnology, University of Helsinki, Finland.

First and foremost, I am grateful and would like to extend my sincere gratitude to my supervisor Frederic Michon for offering me an opportunity to participate in an interesting project to pursue thesis in his group. I am thankful for his patient and his guidance during the project. I am thankful to my coordinator Professor Pirjo Nikula-ljäs, Leila Kauppinen and Professor in-charge of Biochemistry and Biotechnology Department, Professor Kari Keinänen for giving valuable suggestion related to my study.

I am incredibly thankful to my co-supervisor Solja Kalha for her guidance throughout the project and sharing scientific knowledge as well as for giving her valuable comment on my thesis writing. I want to thank all the lab members of Michon lab; Solja Kalha, Kaisa Ikkala, Maria Sanz and Alison kuony for excellent working environment. I want to acknowledge all the members of core facilities of Institute of Biotechnology for helping me with microscopes. My special thanks go to all co-authors of the manuscript Solja Kalha, Maria Sanz, Kyle B Jones and Ophir D Klein.

I would like to thank all my Nepalese friends, who make my stay in Helsinki joyful far from home. Especially, I thank my friends Subhash Shrestha, Yogendra Sangroula and family, Bikesh Raj Upreti and family, Krishna Sangroula and family and Saroj Sitaula. I am lucky to have friends like you all.

Finally, I reserved my thanks to my parent Pradip Krishna Shrestha and Bindira Joshi, my brother and my sister for their constant support. Last but not least, I want to thank my wife Sweta, for being patient in this long journey as well as being inspirational in every possible way. I feel lucky and am immensely thankful to god for having you all around me.

9. ANNEX

Hematoxylin - eosin staining

Deparaffination

1. Xylene 4 minutes x 4
2. ABS ethanol 2 minutes x 3
3. 94 % ethanol 2 minutes x 2
4. 70 % ethanol 2 minutes
5. 50 % ethanol 2 minutes
6. RO - H_2O_2 minutes Staining
7. Hematoxylin 3 minutes
8. Running tap water 3 minutes
9. Eosin 2 minutes

Dehydration

10. 50 % ethanol 15 seconds
11. 70 % ethanol 15 seconds
12. 94 % ethanol 30 seconds x 3
13. ABS ethanol 1-minute x 2
14. ABS ethanol 2 minutes x 2
15. Xylene 2 minutes x 3

Genotyping solutions

Tail lysis buffer

1 M Tris - HCl, pH 8.5

0.5 M EDTA

20 % SDS

5 M NaCl

MQ water

TE buffer

50 mM Tris - HCl, pH 8.0

5 mM EDTA

Cre/ER PCR mix

14,2 µl MQ water

2 µl 10 x Buffer

1,6 µl 2,5 mM dNTP

0,5 µl 10 µM Cre5' primer

0,5 µl 10 µM Cre3' primer

0,2 µl ents. Dynazyme

1 µl template

R26R-LacZ PCR mix

14,1 µl MQ water

2 µl 10 x Buffer

1,6 µl 2,5 mM dNTP

0,5 µl 10 µM 883 primer

0,35 µl 10 µM 316 primer

0,25 µl 10 µM 315 primer

0,2 µl ents. Dynazyme

1 µl template

PCR programs

ROSA-LacZ program

1. 94º C 1 minutes
2. 94º C 30 seconds
3. 60º C 30 seconds
4. 72º C 30 seconds
5. go to step two 35 times

Cre/ER program

1. 95º C 1 minutes
2. 95º C 30 seconds
3. 55º C 1 minutes
4. 72º C 1 minutes
5. 75º C 30 seconds
6. go to step two 40 times
7. 15º C 5 minutes
8. 4º C 10 minutes

Xgal Solutions:

$K_3Fe(CN)_6$ (0,5M) → 1,65g/10ml H2O

$K_4Fe(CN)_6$ (0,5M) → 2,10g/10ml H2OFix: 5 ml 4% PFA

5 ml PBS

80 ml 25% GA

Xgal wash buffer:

2 mM $MgCl_2$, 0.02% NP-40 in PBS

FOR 50ml:

- 2mM $MgCl_2$ (1M) → 0,1ml
- 0,02% NP-40 (10%) → 0,1ml
- PBS → 49,8 ml

X-gal staining solution:

1 mg/ml X-Gal

5 mM $K_3Fe(CN)_6$

5 mM $K_4Fe(CN)_6$, 2 mM $MgCl_2$

0.02% NP-40 for up to E12 or explants

0.1% NP-40

0.2% sodium deoxycholate for E12.5 & older

FOR 10ml:

<u>end c (stock c) → amount to pipet</u>

- 1mg/ml X-gal (50mg/ml) → 0,2 mL
- 5mM $K_3Fe(CN)_6$ (0,5M) → 0,1ml
- 5mM $K_4Fe(CN)_6$ (0,5M) → 0,1ml
- 2mM $MgCl_2$ (1M) → 0,02ml
- 0,1% NP-40 (10%) → 0,1ml
- 0,2% Sodium deoxy (10%) → 0,2ml
- Fill until 10ml with PBS → 9,28ml

Primer sequences

Cre 5'	AAT CTC CCA CCG TCA GTA CG
Cre 3'	CGT TTT CTG AGC ATA CCT GGA
R26F2 forward (883)	AAA GTC GCT CTG AGT TGT TAT
R1295 mut. reverse (315)	GCG AAG AGT TTG TCC TCA ACC
R523 wt. reverse (316)	GGA GCG GGA GAA ATG GAT ATG

10.REFERENCES

Amitai-Lange, A., Altshuler, A., Bubley, J., Dbayat, N., Tiosano, B., & Shalom-Feuerstein, R. (2015). Lineage tracing of stem and progenitor cells of the murine corneal epithelium. *Stem Cells*, *33*(1), 230–239. https://doi.org/10.1002/stem.1840

Auran, J. D., Koester, C. J., Kleiman, N. J., Rapaport, R., Bomann, J. S., Wirotsko, B. M., Florakis, G. J., & Koniarek, J. P. (1995). Scanning Slit Confocal Microscopic Observation of Cell Morphology and Movement within the Normal Human Anterior Cornea. *Ophthalmology*, *102*(1), 33–41. https://doi.org/10.1016/S0161-6420(95)31057-3

Barbaro, V., Testa, A., Di Iorio, E., Mavilio, F., Pellegrini, G., & De Luca, M. (2007). C/EBPδ regulates cell cycle and self-renewal of human limbal stem cells. *Journal of Cell Biology*, *177*(6), 1037–1049. https://doi.org/10.1083/jcb.200703003

Barker, N., Bartfeld, S., & Clevers, H. (2010). Tissue-resident adult stem cell populations of rapidly self-renewing organs. In *Cell Stem Cell* (Vol. 7, Issue 6, pp. 656–670). Cell Press. https://doi.org/10.1016/j.stem.2010.11.016

Beebe, D. C., & Masters, B. R. (1996). Cell lineage and the differentiation of corneal epithelial cells. *Investigative Ophthalmology and Visual Science*, *37*(9), 1815–1825. https://iovs.arvojournals.org/article.aspx?articleid=2161546

Beltrami, A. P., Barlucchi, L., Torella, D., Baker, M., Limana, F., Chimenti, S., Kasahara, H., Rota, M., Musso, E., Urbanek, K., Leri, A., Kajstura, J., & Nadal-Ginard, B. (2003). Adult Cardiac Stem Cells Are Multipotent and Support Myocardial Regeneration we have documented the existence of cycling ventricu- lar myocytes in the normal and pathologic adult mam. *Cell*, *114*(6), 763–776. https://doi.org/10.1016/S0092-8674(03)00687-1

Buck, R. C. (1985). Measurement of centripetal migration of normal corneal epithelial cells in the mouse. *Investigative Ophthalmology and Visual Science*, *26*(9), 1296–1299.

Budak, M. T., Alpdogan, O. S., Zhou, M., Lavker, R. M., Akinci, M. A. M., & Wolosin, J. M. (2005). Ocular surface epithelia contain ABCG2-dependent side population cells exhibiting features associated with stem cells. *Journal of Cell Science*, *118*(8), 1715–1724. https://doi.org/10.1242/jcs.02279

BUSCHKE, W. (1949). Morphologic changes in cells of corneal epithelium in wound healing. *Archives of Ophthalmology*, *41*(3), 306–316. https://doi.org/10.1001/archopht.1949.00900040314003

Chen, J. J., & Tseng, S. C. (1991). Abnormal corneal epithelial wound healing in partial-thickness removal of limbal epithelium. *Investigative Ophthalmology & Visual Science*, *32*(8), 2219–2233. http://www.ncbi.nlm.nih.gov/pubmed/1712763

Chen, J. J. Y., & Tseng, S. C. G. (1990). Corneal epithelial wound healing in partial limbal deficiency. *Investigative Ophthalmology and Visual Science*, *31*(7), 1301–1314. https://iovs.arvojournals.org/article.aspx?articleid=2160290

Chen, W. Y. W., Mui, M. M., Kao, W. W. Y., Liu, C. Y., & Tseng, S. C. G. (1994). Conjunctival epithelial cells do not transdifferentiate in organotypic cultures: Expression of k12 keratin is restricted to corneal epithelium. *Current Eye Research*, *13*(10), 765–778. https://doi.org/10.3109/02713689409047012

Chen, Z., de Paiva, C. S., Luo, L., Kretzer, F. L., Pflugfelder, S. C., & Li, D.-Q. (2004). Characterization of Putative Stem Cell Phenotype in Human Limbal Epithelia. *Stem Cells*, *22*(3), 355–366. https://doi.org/10.1634/stemcells.22-3-355

Chung, E. H., Bukusoglu, G., & Zieske, J. D. (1992). Localization of corneal epithelial stem cells in the developing rat. *Investigative Ophthalmology & Visual Science*, *33*(7), 2199–2206. http://www.ncbi.nlm.nih.gov/entrez/query.fcgi?cmd=Retrieve&db=PubMed&dopt=Citation&list_uids=1607230

Cintron, C., Covington, H., & Kublin, C. L. (1983). Morphogenesis of rabbit corneal stroma. *Invest Ophthalmol Vis Sci*, *24*(5), 543–556. http://www.ncbi.nlm.nih.gov/pubmed/6841000

Collinson, J. M., Morris, L., Reid, A. I., Ramaesh, T., Keighren, M. A., Flockhart, J. H., Hill, R. E., Tan, S.-S., Ramaesh, K., Dhillon, B., & West, J. D. (2002). Clonal analysis of patterns of growth, stem cell activity, and cell movement during the development and maintenance of the murine corneal epithelium. *Developmental Dynamics : An Official Publication of the American Association of Anatomists*, *224*(4), 432–440. https://doi.org/10.1002/dvdy.10124

Collomb, E., Yang, Y., Foriel, S., Cadau, S., Pearton, D. J., & Dhouailly, D. (2013). The corneal epithelium and lens develop independently from a common pool of precursors. *Developmental*

Dynamics, *242*(5), 401–413. https://doi.org/10.1002/dvdy.23925

Cotsarelis, G., Cheng, S. Z., Dong, G., Sun, T. T., & Lavker, R. M. (1989). Existence of slow-cycling limbal epithelial basal cells that can be preferentially stimulated to proliferate: Implications on epithelial stem cells. *Cell*, *57*(2), 201–209. https://doi.org/10.1016/0092-8674(89)90958-6

Davanger, M., & Evensen, A. (1971). © 1971 Nature Publishing Group. *Nature Physical Science*, *231*(5286), 154–155. https://doi.org/10.1038/229560a0

Dhouailly, D., Pearton, D. J., & Michon, F. (2014). The vertebrate corneal epithelium: From early specification to constant renewal. In *Developmental Dynamics* (Vol. 243, Issue 10, pp. 1226–1241). https://doi.org/10.1002/dvdy.24179

Di Girolamo, N., Bobba, S., Raviraj, V., Delic, N. C., Slapetova, I., Nicovich, P. R., Halliday, G. M., Wakefield, D., Whan, R., & Lyons, J. G. (2015). Tracing the fate of limbal epithelial progenitor cells in the murine cornea. *Stem Cells*, *33*(1), 157–169. https://doi.org/10.1002/stem.1769

Di Girolamo, Nick. (2011). Stem cells of the human cornea. *British Medical Bulletin*, *100*(1), 191–207. https://doi.org/10.1093/bmb/ldr026

Dobie, K., Mehtali, M., McClenaghan, M., & Lathe, R. (1997). Variegated gene expression in mice. In *Trends in Genetics* (Vol. 13, Issue 4, pp. 127–130). Clarendon Press in Biochemistry. https://doi.org/10.1016/S0168-9525(97)01097-4

Dominici, M., Le Blanc, K., Mueller, I., Slaper-Cortenbach, I., Marini, F. C., Krause, D. S., Deans, R. J., Keating, A., Prockop, D. J., & Horwitz, E. M. (2006). Minimal criteria for defining multipotent mesenchymal stromal cells. The International Society for Cellular Therapy position statement. *Cytotherapy*, *8*(4), 315–317. https://doi.org/10.1080/14653240600855905

Dorà, N. J., Hill, R. E., Collinson, J. M., & West, J. D. (2015). Lineage tracing in the adult mouse corneal epithelium supports the limbal epithelial stem cell hypothesis with intermittent periods of stem cell quiescence. *Stem Cell Research*, *15*(3), 665–677. https://doi.org/10.1016/j.scr.2015.10.016

Dua, H S, Gomes, J. A. P., & Singh, A. (1994). Corneal epithelial wound healing. *BritishJournal*

OfOphthalmology, *78*(5), 401–408. https://doi.org/10.1136/bjo.78.5.401

Dua, Harminder S., Joseph, A., Shanmuganathan, V. A., & Jones, R. E. (2003). Stem cell differentiation and the effects of deficiency. *Eye*, *17*(8), 877–885. https://doi.org/10.1038/sj.eye.6700573

Dua, Harminder S., Shanmuganathan, V. A., Powell-Richards, A. O., Tighe, P. J., & Joseph, A. (2005). Limbal epithelial crypts: A novel anatomical structure and a putative limbal stem cell niche. *British Journal of Ophthalmology*, *89*(5), 529–532. https://doi.org/10.1136/bjo.2004.049742

Ebato, B., Friend, J., & Thoft, R. A. (1987). Comparison of central and peripheral human corneal epithelium in tissue culture. *Investigative Ophthalmology and Visual Science*, *28*(9), 1450–1456. https://iovs.arvojournals.org/article.aspx?articleid=2159911

Ebato, B., Friend, J., & Thoft, R. A. (1988). Comparison of limbal and peripheral human corneal epithelium in tissue culture. *Investigative Ophthalmology and Visual Science*, *29*(10), 1533–1537. https://iovs.arvojournals.org/article.aspx?articleid=2177894

Eghtedari, Y., Richardson, A., Mai, K., Heng, B., Guillemin, G. J., Wakefield, D., & Di Girolamo, N. (2016). Keratin 14 expression in epithelial progenitor cells of the developing human cornea. *Stem Cells and Development*, *25*(9), 699–711. https://doi.org/10.1089/scd.2016.0039

Evans, M. J., & Kaufman, M. H. (1981). Establishment in culture of pluripotential cells from mouse embryos. *Nature*, *292*(5819), 154–156. https://doi.org/10.1038/292154a0

Fabiani, C., Barabino, S., Rashid, S., & Dana, M. R. (2009). Corneal epithelial proliferation and thickness in a mouse model of dry eye. *Experimental Eye Research*, *89*(2), 166–171. https://doi.org/10.1016/j.exer.2009.03.003

Figueira, E. C., Di Girolamo, N., Coroneo, M. T., & Wakefield, D. (2007). The phenotype of limbal epithelial stem cells. *Investigative Ophthalmology and Visual Science*, *48*(1), 144–156. https://doi.org/10.1167/iovs.06-0346

Friedenstein, A. J., Gorskaja, J. F., & Kulagina, N. N. (1976). Fibroblast precursors in normal and irradiated mouse hematopoietic organs. *Experimental Hematology*, *4*(5), 267–274. http://www.ncbi.nlm.nih.gov/pubmed/976387

Greiling, T. M. S., & Clark, J. I. (2008). The transparent lens and cornea in the mouse and zebra fish eye. In *Seminars in Cell and Developmental Biology* (Vol. 19, Issue 2, pp. 94–99). https://doi.org/10.1016/j.semcdb.2007.10.011

Hambiliki, F., Ström, S., Zhang, P., & Stavreus-Evers, A. (2012). Co-localization of NANOG and OCT4 in human pre-implantation embryos and in human embryonic stem cells. *Journal of Assisted Reproduction and Genetics*, *29*(10), 1021–1028. https://doi.org/10.1007/s10815-012-9824-9

Hass, R., Kasper, C., Böhm, S., & Jacobs, R. (2011). Different populations and sources of human mesenchymal stem cells (MSC): A comparison of adult and neonatal tissue-derived MSC. In *Cell Communication and Signaling* (Vol. 9, Issue 1, p. 12). BioMed Central. https://doi.org/10.1186/1478-811X-9-12

Haustein, J. (1983). On the Ultrastructure of the Developing and Adult Mouse Corneal Stroma. *Anat Embryol*, *168*(2), 291–305. https://doi.org/10.1007/BF00315823

Hay, E. D. (1980). Development of the Vertebrate Cornea. *International Review of Cytology*, *63*(C), 263–322. https://doi.org/10.1016/S0074-7696(08)61760-X

Higa, K., Shimmura, S., Miyashita, H., Kato, N., Ogawa, Y., Kawakita, T., Shimazaki, J., & Tsubota, K. (2009). N-Cadherin in the maintenance of human corneal limbal epithelial progenitor cells in vitro. *Investigative Ophthalmology and Visual Science*, *50*(10), 4640–4645. https://doi.org/10.1167/iovs.09-3503

Huang, A. J. W., & Tseng, S. C. G. (1991). Corneal epithelial wound healing in the absence of limbal epithelium. *Investigative Ophthalmology and Visual Science*, *32*(1), 96–105. http://www.ncbi.nlm.nih.gov/pubmed/1702774

Kasper, M, Moll, R., Stosiek, P., & Karsten, U. (1988). Histochemistry Patterns of cytokeratin and vimentin expression in the human eye. In *Histochemistry* (Vol. 89).

Kasper, Michael. (1992). Patterns of cytokeratins and vimentin in guinea pig and mouse eye tissue: Evidence for regional variations in intermediate filament expression in limbal epith. *Acta Histochemica*, *93*(1), 319–332. https://doi.org/10.1016/S0065-1281(11)80231-X

Katikireddy, K. R., Dana, R., & Jurkunas, U. V. (2014). Differentiation potential of limbal

fibroblasts and bone marrow mesenchymal stem cells to corneal epithelial cells. *Stem Cells*, *32*(3), 717–729. https://doi.org/10.1002/stem.1541

Kayama, M., Kurokawa, M. S., Ueno, H., & Suzuki, N. (2007). Recent advances in corneal regeneration and possible application of embryonic stem cell-derived corneal epithelial cells. *Clinical Ophthalmology (Auckland, N.Z.)*, *1*(4), 373–382.

Kenyon, K. R., & Tseng, S. C. (1989). Limbal autograft transplantation for ocular surface disorders. *Ophthalmology*, *96*(5), 709–722; discussion 722-3. http://www.ncbi.nlm.nih.gov/pubmed/2748125

Kolozsvári, L., Nógrádi, A., Hopp, B., & Bor, Z. (2002). UV absorbance of the human cornea in the 240- to 400-nm range. *Investigative Ophthalmology and Visual Science*, *43*(7), 2165–2168.

Ksander, B. R., Kolovou, P. E., Wilson, B. J., Saab, K. R., Guo, Q., Ma, J., McGuire, S. P., Gregory, M. S., Vincent, W. J. B., Perez, V. L., Cruz-Guilloty, F., Kao, W. W. Y., Call, M. K., Tucker, B. A., Zhan, Q., Murphy, G. F., Lathrop, K. L., Alt, C., Mortensen, L. J., … Frank, N. Y. (2014). ABCB5 is a limbal stem cell gene required for corneal development and repair. *Nature*, *511*(7509), 353–357. https://doi.org/10.1038/nature13426

Kurpakus, M. A., Stock, E. L., & Jones, J. C. R. (1990). Expression of the 55-kD/64-kD corneal keratins in ocular surface epithelium. *Investigative Ophthalmology and Visual Science*, *31*(3), 448–456.

Lauweryns, B., Van den Oord, J. J., & Missotten, L. (1993). The transitional zone between limbus and peripheral cornea: An immunohistochemical study. *Investigative Ophthalmology and Visual Science*, *34*(6), 1991–1999.

Lehrer, M. S., Sun, T. T., & Lavker, R. M. (1998). Strategies of epithelial repair: Modulation of stem cell and transit amplifying cell proliferation. *Journal of Cell Science*, *111*(19), 2867–2875. https://jcs.biologists.org/content/111/19/2867.long

Levis, H. J., & Daniels, J. T. (2016). Recreating the Human Limbal Epithelial Stem Cell Niche with Bioengineered Limbal Crypts. *Current Eye Research*, *41*(9), 1153–1160. https://doi.org/10.3109/02713683.2015.1095932

Lindberg, K., Brown, M. E., Chaves, H. V., Kenyon, K. R., & Rheinwald, J. G. (1993). In vitro

propagation of human ocular surface epithelial cells for transplantation. *Investigative Ophthalmology and Visual Science*, *34*(9), 2672–2679. https://iovs.arvojournals.org/article.aspx?articleid=2161000

Liu, C. Y., Zhu, G., Westerhausen-Larson, A., Converse, R., Candace, W. C. K., Sun, T. T., & Winston, W. Y. K. (1993). Cornea-specific expression of k12 keratin during mouse development. *Current Eye Research*, *12*(11), 963–974. https://doi.org/10.3109/02713689309029222

Majo, F., Rochat, A., Nicolas, M., Jaoudé, G. A., & Barrandon, Y. (2008a). Oligopotent stem cells are distributed throughout the mammalian ocular surface. *Nature*, *456*(7219), 250–254. https://doi.org/10.1038/nature07406

Majo, F., Rochat, A., Nicolas, M., Jaoudé, G. A., & Barrandon, Y. (2008b). Oligopotent stem cells are distributed throughout the mammalian ocular surface. *Nature*, *456*(7219), 250–254. https://doi.org/10.1038/nature07406

Mann, I. (1944). a Study of Epithelial Regeneration in the Living Eye. *The British Journal of Ophthalmology*, *28*(1902), 26–40. https://doi.org/10.1136/bjo.28.1.26

Martin, G. R. (1981). Isolation of a pluripotent cell line from early mouse embryos cultured in medium conditioned by teratocarcinoma stem cells. *Proceedings of the National Academy of Sciences*, *78*(12).

Mei, H., Nakatsu, M. N., Baclagon, E. R., & Deng, S. X. (2014). Frizzled 7 maintains the undifferentiated state of human limbal stem/progenitor cells. *Stem Cells*, *32*(4), 938–945. https://doi.org/10.1002/stem.1582

Moll, R., Franke, W. W., Schiller, D. L., Geiger, B., & Krepler, R. (1982). The catalog of human cytokeratins: Patterns of expression in normal epithelia, tumors and cultured cells. In *Cell* (Vol. 31, Issue 1, pp. 11–24). https://doi.org/10.1016/0092-8674(82)90400-7

Molofsky, A. V., Pardal, R., Iwashita, T., Park, I. K., Clarke, M. F., & Morrison, S. J. (2003). Bmi-1 dependence distinguishes neural stem cell self-renewal from progenitor proliferation. *Nature*, *425*(6961), 962–967. https://doi.org/10.1038/nature02060

Pajoohesh-Ganji, A., Ghosh, S. P., & Stepp, M. A. (2004). Regional distribution of α9β1 integrin

within the limbus of the mouse ocular surface. *Developmental Dynamics*, *230*(3), 518–528. https://doi.org/10.1002/dvdy.20050

Park, I. K., Qian, D., Kiel, M., Becker, M. W., Pihalja, M., Weissman, I. L., Morrison, S. J., & Clarke, M. F. (2003). Bmi-1 is required for maintenance of adult self-renewing haematopoietic stem cells. *Nature*, *423*(6937), 302–305. https://doi.org/10.1038/nature01587

Pellegrini, G., Dellambra, E., Golisano, O., Martinelli, E., Fantozzi, I., Bondanza, S., Ponzin, D., McKeon, F., & De Luca, M. (2001). p63 identifies keratinocyte stem cells. *Proceedings of the National Academy of Sciences of the United States of America*, *98*(6), 3156–3161. https://doi.org/10.1073/pnas.061032098

Pellegrini, G., Golisano, O., Paterna, P., Lambiase, A., Bonini, S., Rama, P., & De Luca, M. (1999). Location and clonal analysis of stem cells and their differentiated progeny in the human ocular surface. *The Journal of Cell Biology*, *145*(4), 769–782. https://doi.org/10.1083/jcb.145.4.769

Pispa, J., Pummila, M., Barker, P. A., Thesleff, I., & Mikkola, M. L. (2008). Edar and Troy signalling pathways act redundantly to regulate initiation of hair follicle development. *Human Molecular Genetics*, *17*(21), 3380–3391. https://doi.org/10.1093/hmg/ddn232

Polisetty, N., Fatima, A., Madhira, S. L., Sangwan, V. S., & Vemuganti, G. K. (2008). Mesenchymal cells from limbal stroma of human eye. *Molecular Vision*, *14*, 431–442. https://doi.org/v14/a53 [pii]

Rheinwald, J. G., & Green, H. (1975). Formation of a keratinizing epithelium in culture by a cloned cell line derived from a teratoma. *Cell*, *6*(3), 317–330. https://doi.org/10.1016/0092-8674(75)90183-X

Rodrigues, M., Ben-Zvi, A., Krachmer, J., Schermer, A., & Sun, T. T. (1987). Suprabasal expression of a 64-kilodalton keratin (no. 3) in developing human corneal epithelium. *Differentiation*, *34*(1), 60–67. https://doi.org/10.1111/j.1432-0436.1987.tb00051.x

Sartaj, R., Zhang, C., Wan, P., Pasha, Z., Guaiquil, V., Liu, A., Liu, J., Luo, Y., Fuchs, E., & Rosenblatt, M. I. (2017). Characterization of slow cycling corneal limbal epithelial cells identifies putative stem cell markers. *Scientific Reports*, *7*(1), 1–14. https://doi.org/10.1038/s41598-017-04006-y

Schermer, A., Galvin, S., & Sun, T.-T. T. (1986). Differentiation-related expression of a major 64K corneal keratin in vivo and in culture suggests limbal location of corneal epithelial stem cells. *Journal of Cell Biology*, *103*(1), 49–62. https://doi.org/10.1083/jcb.103.1.49

Shanmuganathan, V. A., Foster, T., Kulkarni, B. B., Hopkinson, A., Gray, T., Powe, D. G., Lowe, J., & Dua, H. S. (2007). Morphological characteristics of the limbal epithelial crypt. *British Journal of Ophthalmology*, *91*(4), 514–519. https://doi.org/10.1136/bjo.2006.102640

Shortt, A. J., Secker, G. A., Munro, P. M., Khaw, P. T., Tuft, S. J., & Daniels, J. T. (2007). Characterization of the Limbal Epithelial Stem Cell Niche: Novel Imaging Techniques Permit In Vivo Observation and Targeted Biopsy of Limbal Epithelial Stem Cells. *Stem Cells*, *25*(6), 1402–1409. https://doi.org/10.1634/stemcells.2006-0580

Tanifuji-Terai, N., Terai, K., Hayashi, Y., Chikama, T. I., & Kao, W. W. Y. (2006). Expression of keratin 12 and maturation of corneal epithelium during development and postnatal growth. *Investigative Ophthalmology and Visual Science*, *47*(2), 545–551. https://doi.org/10.1167/iovs.05-1182

Thoft, R., Friend, J., Jm, E., E, A., F, F., E, G., H, H., & G, V. (1983). The X , Y , Z Hypothesis of Comeol Epitheliol Mointenonce To the Editor : For the past few years , studies of corneal epithelial of corneal epithelial disease . Department of Ophthalmology. *Investigative Ophthalmology & Visual Science*, *24*(October), 1442–1443.

Thomas, P. B., Liu, Y. H., Zhuang, F. F., Selvam, S., Song, S. W., Smith, R. E., Trousdale, M. D., & Yiu, S. C. (2007). Identification of Notch-1 expression in the limbal basal epithelium. *Molecular Vision*, *13*, 337–344. /pmc/articles/PMC2633467/?report=abstract

Tsai, R. J. F., Sun, T. T., & Tseng, S. C. G. (1990). Comparison of Limbal and Conjunctival Autograft Transplantation in Corneal Surface Reconstruction in Rabbits. *Ophthalmology*, *97*(4), 446–455. https://doi.org/10.1016/S0161-6420(90)32575-7

Tseng, S. C. G., & Tsai, R. J. F. (1991). Limbal transplantation for ocular surface reconstruction - A review. *Fortschritte Der Ophthalmologie*, *88*(3), 236–242. http://www.ncbi.nlm.nih.gov/pubmed/1889770

Umemoto, T., Yamato, M., Nishida, K., Yang, J., Tano, Y., & Okano, T. (2006). Limbal Epithelial Side-Population Cells Have Stem Cell-Like Properties, Including Quiescent State. *Stem Cells*,

24(1), 86–94. https://doi.org/10.1634/stemcells.2005-0064

Valiente-Alandi, I., Albo-Castellanos, C., Herrero, D., Arza, E., Garcia-Gomez, M., Segovia, J. C., Capecchi, M., & Bernad, A. (2015). Cardiac *Bmi1*+cells contribute to myocardial renewal in the murine adult heart. *Stem Cell Research and Therapy*, *6*(1). https://doi.org/10.1186/s13287-015-0196-9

Wang, D. Y., Hsueh, Y. J., Yang, V. C., & Chen, J. K. (2003). Propagation and Phenotypic Preservation of Rabbit Limbal Epithelial Cells on Anmiotic Membrane. *Investigative Ophthalmology and Visual Science*, *44*(11), 4698–4704. https://doi.org/10.1167/iovs.03-0272

Wei, Z. G., Wu, R. L., Lavker, R. M., & Sun, T. T. (1993). In vitro growth and differentiation of rabbit bulbar, fornix, and palpebral conjunctival epithelia: Implications on conjunctival epithelial transdifferentiation and stem cells. *Investigative Ophthalmology and Visual Science*, *34*(5), 1814–1828. https://iovs.arvojournals.org/article.aspx?articleid=2179215

Williams, R. L., Hilton, D. J., Pease, S., Willson, T. A., Stewart, C. L., Gearing, D. P., Wagner, E. F., Metcalf, D., Nicola, N. A., & Gough, N. M. (1988). Myeloid leukaemia inhibitory factor maintains the developmental potential of embryonic stem cells. *Nature*, *336*(6200), 684–687. https://doi.org/10.1038/336684a0

Yan, K., Chia, L., & Li, X. (2012). The intestinal stem cell markers *Bmi1* and Lgr5 identify two functionally distinct populations. *Pnas*, *109*(2), 466–471. https://doi.org/10.1073/pnas.1118857109/-/DCSupplemental.www.pnas.org/cgi/doi/10.1073/pnas.1118857109

Yoshida, S., Shimmura, S., Kawakita, T., Miyashita, H., Den, S., Shimazaki, J., & Tsubota, K. (2006). Cytokeratin 15 can be used to identify the limbal phenotype in normal and diseased ocular surfaces. *Investigative Ophthalmology and Visual Science*, *47*(11), 4780–4786. https://doi.org/10.1167/iovs.06-0574

Zieske, J. D. (2004). Corneal development associated with eyelid opening. In *International Journal of Developmental Biology* (Vol. 48, Issues 8–9, pp. 903–911). https://doi.org/10.1387/ijdb.041860jz

ARTICLE

Bmi1+ progenitor cell dynamics during the murine corneal maturation, renewal and wound healing

Solja Kalha[a], Bideep Shrestha[a], Maria Sanz Navarro[a], Kyle Jones[b], Ophir D. Klein[b,c] and Frederic Michon[a*]

[a]Institute of Biotechnology, Developmental Biology Program, University of Helsinki, 00014, Helsinki, Finland.

[b]Department of Orofacial Sciences and Program in Craniofacial Biology, UCSF, San Francisco, USA

[c]Department of Pediatrics and Institute for Human Genetics, University of California San Francisco, San Francisco, CA 94143, USA

*Corresponding author: Frederic Michon, Ph.D., Institute of Biotechnology, University of Helsinki, Viikinkaari 5 00790 Helsinki, Finland. frederic.michon@helsinki.fi

Author contributions:

Solja Kalha: conception and design, collection and assembly of data, data analysis and interpretation, manuscript writing

Bideep Shrestha: collection and assembly of data

Maria Sanz Navarro: collection and assembly of data

Kyle Jones: conception and design

Ophir Klein: conception and design, manuscript writing, final approval of manuscript

Frederic Michon: conception and design, data analysis and interpretation, manuscript writing, final approval of manuscript

Keywords: cornea, Bmi1, stem cell, progenitor, maturation, renewal, wound healing

Running head: *Bmi1+* progenitors in the murine corneal renewal

Abstract

The outermost layer of the eye, the cornea, is renewed continuously throughout life. Stem cells of the corneal epithelium reside in the limbus at the corneal periphery. These stem cells replenish the cornea from limbus towards the central cornea forming stripes. In young mice, the limbal stripes have not formed yet, but the epithelium renews itself from the basal layer to the superficial layer. We studied the transition from a newborn to an adult state in the aspects of growth and keratin 19 (*Krt19*) expression, as a hallmark of corneal maturation. In addition, we sought for a novel marker of murine corneal epithelial progenitor cells before, during and after maturation. We found that *Bmi1* (polycomb ring finger oncogene) is expressed in the basal epithelium of the central cornea and limbus. Furthermore, we followed the *Bmi1+* cells by genetic fate mapping and demonstrated that *Bmi1+* cells participated in tissue replenishment in the central cornea. However, *Bmi1+* cells did not maintain the cornea for long-term and they did not contribute to the formation of limbal stripes. This data suggests that they are progenitors, rather than stem cells. After an injury, *Bmi1+* cells continued homeostatic maintenance and wound healing occurred via epithelial reorganization. This study introduces the role of *Bmi1* in the mouse cornea and dissects the steps of corneal maturation in detail.

Graphical abstract

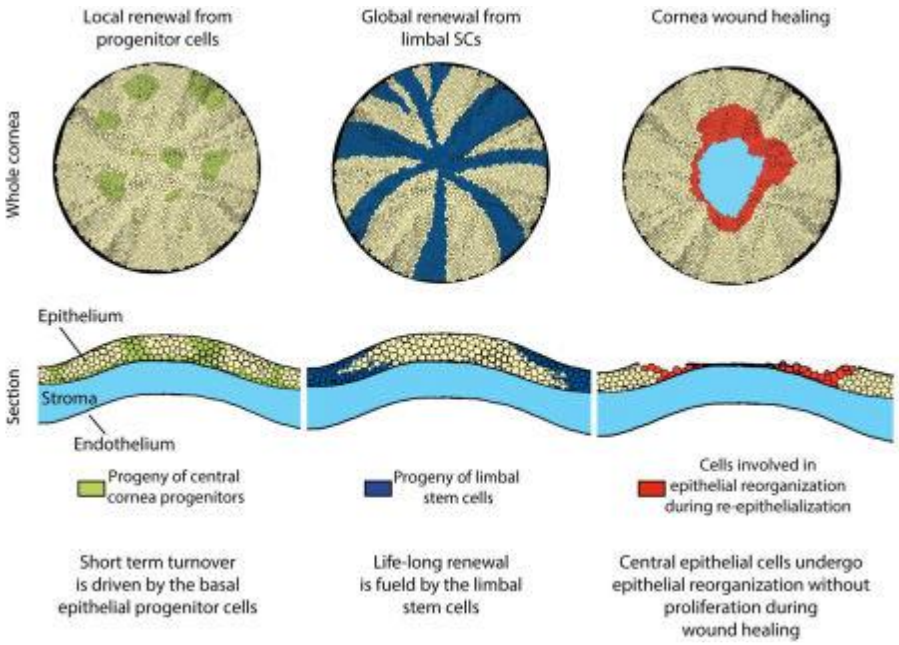

Introduction

The cornea is the transparent layer that covers the surface of the eye. It serves as a barrier to pathogens and water loss, and forms a refractive layer essential for vision. The outermost layer is formed by the corneal epithelium, where cells are strictly adherent to each other and in contact with the physical environment. Basal epithelial cells sit on the basement membrane. Suprabasal and superficial epithelial cells make up the following 3-4 cell layers and the superficial layer faces the tear film; a source of hydration and nutrients to the epithelium. In mice, cornea matures to its adult morphology postnatally. Mice open their eyelids around postnatal day 14 (P14), concomitantly with the beginning of epithelial stratification [1]. The epithelium is fully stratified by P21.

Corneal epithelium is renewed throughout life. Stem cells that fuel this renewal are situated in the periphery of the cornea, in a ring-like structure called the limbus [2]. Early work identified label retaining cells (LRCs) of the cornea in the limbus, suggesting that this is the stem cell niche of the cornea [3,4]. Several studies have shown centripetal renewal of the corneal epithelium from the limbus to the central cornea using genetic fate mapping [5–8]. However, renewal patterns exhibit temporal and species-specific differences [9]. Collinson et al. first showed, that in mouse, limbal renewal only begins at around 5 weeks of age [5]. Before that, the central corneal epithelial cells renew locally [5], quite similar to epidermal proliferative units in skin [10]. Genetic fate mapping showed that central corneal renewal is a temporary phenomenon; stripes originating from the limbus replace the central corneal cell clusters by 10-14 weeks of age [5,6].

Several groups have proposed different markers for epithelial stem cells in the adult cornea. The expression of a previously identified stem cell marker, *Bmi1*, was detected in the human limbus together with *C/EBPδ* [11]. *Bmi1* expression was later confirmed in an *in vitro* model on naïve human limbal epithelial cells and limbal holoclones from pig [12,13]. *Bmi1* is of particular interest because it is expressed in stem cells of several organs, including the bone marrow, central and peripheral

nervous systems, intestine and the tooth [14–18]. In these tissues, *Bmi1* functions in stem cell self-renewal [14–16] and regeneration after injury [19]. Studies on *Bmi1* deficient mice have shown that the absence of *Bmi1* results in severe defects in skeletal patterning, intestinal development and hematopoiesis [15,20,21]. These defects are likely a result of oxidative damage in $Bmi1^{-/-}$ cells [22]. Thus, the identification of *Bmi1* expression in the cornea provides an intriguing avenue into studying stem cells and renewal of the corneal epithelium.

As the ocular surface is an exposed tissue, it is regularly challenged by physical damage. Wound healing studies have been combined with genetic fate mapping of epithelial cells, using *Krt14* as a driver for reporter expression [7]. This study employed a chemical wound and showed that the limbal contribution in wound healing increases with the severity of the wound, whereas mild wounds do not require limbal input for healing. In contrast, Majo et al., challenged the concept of limbal renewal and showed that the central cornea houses cells that are able to repopulate the ocular surface upon injury [13]. However, as genetic fate mapping from a defined stem cell population in homeostasis and injury are still missing, it is difficult to dissect the identity of these cells. The difference between corneal renewal pattern in mouse and other species might lie in the differential timing of corneal maturation. It is not fully understood, where and when the limbal stem cells (LSCs) are first established in the mouse, which could contribute to the differences in lineage tracing after injury. Thus, it is important to consider the age of the mouse and the role of cornea and eye growth in this process.

In this study, we identified a novel marker of murine corneal epithelial progenitor cells, *Bmi1*, and we addressed the usability of this marker in studying cornea renewal. We studied cornea maturation in detail and characterized *Krt19* in the maturation process. Furthermore, we showed that *Bmi1* is expressed at similar levels throughout the animal's life. We found that *Bmi1* localized to the basal epithelium in the central cornea and limbus. Together with the rest of basal epithelium, *Bmi1*+ cells participated in tissue renewal in the central cornea. Interestingly, genetic fate mapping demonstrated

that *Bmi1+* cells were progenitor cells that were replaced after 6 to 8 weeks, and after injury, *Bmi1+* cells were not involved in wound healing. Taken together, these observations showed that the central cornea harbors cells that regularly act as progenitors, but have a limited life span.

Materials and methods

Animals

If not otherwise indicated, we used outbred NMRI mice in our experiments. For the label retaining experiment, we used outbred ICR mice. The generation and characterization of $Bmi1^{CreERT}$ and $R26R^{LacZ}$ mice have been described earlier [17,23]. Both lines were maintained in outbred NMRI background, but crossed with each other to obtain $Bmi1^{CreERT/wt}$;$R26R^{LacZ/wt}$ animals for genetic inducible fate mapping. Vaginal plug day was counted as embryonic day (E) 0.5. Postnatal days are numbered from the date of birth (P0). All animal experiments were approved by the national Animal Experiment Board.

Histology and immunostaining

Mouse tissues (eyeballs or whole heads) were fixed in 4 % PFA (paraformaldehyde), dehydrated, and embedded in paraffin. E18.5 head samples were decalcified with 0.5 M EDTA (ethylenediaminetetra acetic acid) for two weeks before paraffin embedding. 5µm-thick paraffin sections were stained with hematoxylin (Sigma-Aldrich) and eosin (Sigma-Aldrich). For immunofluorescence, sections were pretreated for clearing and rehydration, followed by antigen retrieval for two hours in a pressure cooker (Retriever 2100, Aptum Biologics), immersed in 10 mM sodium citrate buffer. Retrieval was followed by preblocking with 3 % hydrogen peroxide (Sigma-Aldrich) in methanol (Sigma-Aldrich) and tissue permeabilization with 0.3 % Triton-X in PBS. After antigen blocking with 10 % serum in 1 % BSA (bovine serum albumin) in PBS, sections were incubated overnight with a primary antibody in the blocking solution. We used antibodies for Keratin 19 (Abcam, ab52625) and β-catenin (BD Biosciences, 610154) in 1:100 and Ki67 (Abcam, ab16667) in 1:200 concentrations, followed by Alexa 488 or 568 -conjugated secondary antibodies (Thermo Scientific, A11008 or A10042) and Hoechst (Thermo Scientific) counterstaining. For immunostaining on Bmi1 (1:200, Cell Signaling, 6964S), we used abovementioned pretreatments, followed by preblocking; 1 % hydrogen peroxide in methanol and tissue permeabilization as above. Samples were blocked using 3 % BSA, 20 mM

$MgCl_2$, 0.3 % Tween-20 (Sigma-Aldrich) and 5 % FBS (fetal bovine serum) (Hyclone, GE Healthcare) in PBS. Primary antibody was incubated overnight in the blocking solution and subsequently in an anti-rabbit HRP-conjugated secondary antibody (ImmunoLogic). We performed a 3,3-diaminobenzidine staining (Vector Laboratories) and used 50% Gills Hematoxylin (Sigma-Aldrich) for counterstaining.

Eye size measurements and quantification of *Ki67+* corneal epithelial cells

Eye sizes were measured from fresh, enucleated eyes (n=3-7/time point). Measurements were done using the ZEN software (blue edition, 2009-2011, 1.0.0.0., Carl Zeiss). Growth categories were based on statistical difference between age pairs as follows: intense ($p \leq 0.05$ between adjacent age pairs), moderate ($p \leq 0.05$ between non-adjacent age pairs) or no growth (size differences between ages did not differ statistically). *Ki67+* cells were counted manually after immunostaining on 20 serial sections (5µm intervals) from 3 different individuals. Each corneal epithelium was divided into two limbal, two peripheral and one central compartment that encompass 6.4 % (2x), 14.6 % (2x) and 58 % of the epithelium, respectively (Supporting Information Fig. S1A), using the ZEN software (blue edition, 2009-2011, 1.0.0.0., Carl Zeiss). *Ki67+* cells were calculated separately for each compartment and then normalized to the area (A) of the compartment by using the formula *Ki67+* cells/(Ax5x20). Coverage of the cornea was calculated with π x (($\sqrt{cornea}\, r$) + ($\sqrt{cornea}\, height$))/4 x π x ($\sqrt{eye}\, r$).

***In situ* RNA hybridization**

In situ RNA hybridization was performed using RNAscope technology (Advanced Cell Diagnostics), following a manufacturer's protocol. We used a mouse *Bmi1* probe (target region 3096 – 3549 of NM_007552.4) and a colorimetric revelation kit (Advanced Cells Diagnostics). Sections were photographed using an Olympus AX70 microscope.

Genetic inducible fate mapping

For genetic fate mapping of *Bmi1+* cells in embryonic stages, pregnant females were injected (i.p.) twice with tamoxifen (Sigma-Aldrich). At P4 and P5, mice were injected (i.p.) twice with tamoxifen (Sigma-Aldrich) and from the age of 4 weeks onwards, tamoxifen administration route was oral (i.g.), and given on two consecutive days. Tamoxifen was prepared at 50mg/ml in corn oil (Sigma-Aldrich) and given at the daily dose of 10mg/30 g at all stages. X-Gal staining was performed as previously described [24] and sections were counterstained with Nuclear FAST red (Fluka) supplemented with thymol (Sigma-Aldrich). Sections were photographed with an Olympus AX70 microscope.

Labeling and detecting label retaining cells

We gave a single injection of 5-bromo-2'-deoxyuridine (BrdU, GE Healthcare) at 0,6 mg/animal to label cycling cells. BrdU staining followed the abovementioned immunofluorescent staining protocol, excluding methanol blocking. We used anti-BrdU antibody (1:400, GE Healthcare, RPN202).

Cornea injury model

We used 4 weeks old mice for the initial cornea injury model. Injuries were performed in aenesthesia, using ketamine-medetomidine, 75 mg/kg + 1 mg/kg (i.p.) (Orion Pharma, Intervet). First, we scraped away a circular area of the central cornea with Algerbrush 2, BR2-5 0.5 mm (Alger Company). We took care not to injure peripheral and limbal regions. After this, we stained the ocular surface with 0.1 % fluorescein (Sigma-Aldrich) and photographed it under cobalt blue light with a Nikon SLR camera. We finished the experiment by administering the animals with analgesics; buprenorphine, 0.05-0.1 mg/kg, (i.p.) (Invidior), and an impulse; atipamezol 0.5 mg/kg, (i.p.) (Orion Pharma). We gave experimental animals' carprofen, 5 mg/kg (i.p.) (Norbrook) and eye ointment (Isathal) daily until sacrifice. In addition, we used $Bmi1^{CreERT/wt}$;$R26R^{LacZ/wt}$ animals for an experiment where cornea injury was combined with genetic fate mapping experiment. Cre activation was induced as described above at the age of 6 weeks. We performed the injury two weeks later, as described in this section. Eyes were enucleated and processed for X-gal staining and then imaged with Zeiss Lumar

stereomicroscope. The right eye was not scraped in neither case and thus served as a control. We estimated the epithelial thickness after wounding from hematoxylin and eosin stained sections. Thickness was measured from 3 wounded and 3 bilateral, unwounded eye sections using the ZEN software (blue edition, 2009-2011, 1.0.0.0., Carl Zeiss). Measurements were always taken from the largest possible region in the central cornea. Furthermore, we took measurements from wounded and unwounded pairs from an area that corresponded to each other in distance to the limbus.

Statistics

Eye and cornea size measurements, *Ki67+* cell quantification and epithelial thickness after injury was tested statistically using SPSS Statistics 22 for ANOVA (analysis of variance), combined with Tukey or Bonferroni post hoc tests and, when needed, with Kruskal-Wallis test with pairwise comparisons. We used $p \leq 0.05$ as significant.

Results

The identity of the limbus is set before cornea reaches adult size

We hypothesized that the gradual switch in keratin expression pattern in mouse reflected the pace of corneal maturation. Therefore, to evaluate the chronological events that lead to the formation of a limbal stem cell niche, we investigated expression patterns of *Krt19* in young and adult mouse cornea. *Krt19* expression was previously studied in the basal epithelium of the adult human and mouse limbus [25–28]. We followed *Krt19*+ cells during cornea morphogenesis. While we detected *Krt19* expression in the entire embryonic corneal epithelium, from E13.5 to E18.5 (data not shown), the postnatal expression pattern changed progressively. Immediately after birth, *Krt19* was homogeneously expressed in the epithelium (Fig. 1A-A’’’). Already at P7, we detected regions in the central cornea that were devoid of *Krt19*+ cells (Fig. 1B’), but all limbal cells still expressed it (Fig. 1B’’-B’’’). After P7, when corneal epithelial stratification begins, *Krt19* expression gradually decreased from the central and peripheral cornea (Fig. 1C-C’) until it was totally lost by P21 (Fig. 1D-D’). Thereafter, *Krt19* expression pattern was similar to the one found in adult mice (Fig. 1E-E’’’). Our results demonstrated the progressive, postnatal maturation of the cornea and the rapid emergence of the limbus as the corneal stem cell niche after eyelid opening.

To understand if the process of corneal maturation was concomitant with a change in the eye morphology, we analyzed the growth of the mouse eyeball and cornea. We assorted the growth patterns to three categories; intense, moderate or no growth. As highlighted from the measurements, the most intense period of growth occurred during the first postnatal week, but the eyeball continued steady growing until the age of 4 weeks (Fig. 1F). After 4 weeks of age, the eyeball did not grow significantly anymore. Additionally, our measurements pointed out that the area covered by the cornea expanded as well. At birth, the mouse cornea covered 18 % of the eyeball. By one year of age, the coverage increased up to 37 %. Interestingly, the mouse cornea growth pace was dissimilar to the

one of the eyeball. The cornea underwent two waves of intense growth. The first one was simultaneous with the intense growth period of the eyeball during the first week after birth. The second period of intense growth happened after the eyelid opening and the stratification of the cornea, between P21 and 4 weeks of age (Fig. 1G). Both waves were followed by a period of moderate growth (Fig. 1G). The cornea reached adult size by 16 weeks of age (Fig. 1G), long after the eyeball had stopped growing.

When we analyzed the input of proliferating cells on cornea growth, we quantified *Ki67+* cells in the mouse corneal epithelium from P0 to 24 weeks of age (Fig 1H). *Ki67+* cells were detected in the limbus, peripheral cornea and central cornea at all ages (Supporting Information Fig. S1B). The quantity of *Ki67+* cells/μm^3 was maintained at a steady level relative to the size of the cornea, increasing as the cornea grew larger (Fig. 1H). Our observations showed a constant rate of cell proliferation; sustaining first the cornea growth, then stratification, and finally constant renewal. Collectively, these results demonstrated the chronology of the stem cell niche formation, maturation of the cornea, and constant proliferation sustaining tissue growth.

Bmi1 expression is found early in the developing murine cornea

Next, we wanted to look deeper into the developmental expression patterns of other interesting genes. Previous studies had shown that the expression of *Bmi1* followed that of known limbal markers, *p63* and Keratin 15 (*Krt15*), in the adult human cornea [11,29]. Notably, *p63* and *Krt15* become restricted to the human limbus already before birth [29]. Therefore, we investigated *Bmi1* expression and the fate of *Bmi1+* cells during cornea morphogenesis. We detected prominent expression of *Bmi1* from E12.5 until E18.5 throughout the corneal epithelium (Supporting Information Fig. S2). As *Bmi1* expression was previously reported to be limited to the limbus in adult human cornea [11], we investigated if the differential timeline of cornea maturation in mice had an influence on *Bmi1* expression pattern. We saw BMI1 in basal and suprabasal epithelial layers before epithelial stratification (Fig. 2A-B’’’) and in all layers after stratification at P14 (Fig. 2C-C’’’). However,

already at P14, some of the epithelial cells lost *Bmi1* expression, and it became more restricted to the basal epithelium by P21 (Fig. 2D-D'''). We performed an inducible genetic fate mapping experiment starting from P4 and observed the generation of epithelial clones and stripes from *Bmi1*+ cells after over two weeks of chase (Supporting Information Fig. S3). Thus, *Bmi1*+ cells participated actively in cornea growth during maturation.

Bmi1+ cells are corneal epithelial progenitor cells

As the expression of *Bmi1* seemed broader than expected from a stem cell population, we investigated *Bmi1*+ cells in the maturing and fully matured mouse cornea. We used immunostaining and highly sensitive RNA *in situ* hybridization to visualize subtle changes in *Bmi1* expression. Unexpectedly, we did not detect any change of *Bmi1* expression pattern at the protein or RNA levels over time (Fig. 3). Almost all basal epithelial cells were *Bmi1*+, while few suprabasal cells expressed *Bmi1* (Fig. 3A, A', B, B', C, C', D, D'). Notably, we detected some *Bmi1*-negative cells scattered in the basal layer of the central cornea (Fig. 3A, A', A''', B'', B''', C, C'', D''').

Next, we analyzed participation of the *Bmi1*+ cells in cornea renewal. The inducible genetic fate mapping revealed a peculiar pattern of corneal renewal (Fig. 4). First, we studied the progeny of *Bmi1*+ cells in 1 month old animals, which have a recently matured cornea. The *Bmi1*+ cell progeny arose in clusters, displaying a patchy pattern in central, peripheral and limbal cornea two weeks after induction (Fig. 4B-B'). The cluster remained until 4 weeks of chase (Fig. 4C-C'), but disappeared at 8 weeks (Fig. 4D-D'). However, rare stripes from the peripheral cornea formed at 8 weeks and withheld until 16 weeks of chase (Fig. 4F-F'). By 20 weeks of chase, we no longer detected the progeny of the labelled *Bmi1*+ cells. (Fig. 4G-G'). Long-term follow up of corneal renewal did not show persistent or new generation of epithelial cells from the originally labelled *Bmi1*+ cells (Fig. 4H-I). Histological analysis showed that the described clusters arose from single *Bmi1*+ cells (Fig. 4J-J''). *Bmi1*+ clones grew larger with longer time intervals and expanded sideways, also in the basal layer (Fig. 4K'). Then, to understand if these observations were age-dependent, we applied the same

approach to older animals. We conducted the second part of the fate mapping experiment using 6 month old mice (Fig. 5A). In this experiment, we observed rare, small, *Bmi1+* cell clusters after four and eight weeks of chase (Fig. 5A-E). These clusters disappeared upon longer chase times. The observation that *Bmi1* is expressed throughout the basal layer but X-gal is not staining an even area in the entire cornea, showing the *Bmi1+* cells and their progeny, suggests that the recombination efficiency is low, but within a normal range [30]. Our results are in line with the previous report on mouse cornea; the epithelial renewal decreases upon aging [6]. The progressive loss of *Bmi1+* cell progeny in fate mapping led us to assess the distribution of *Ki67+* cells and LRCs in the cornea. Our results clearly indicated, that the *Bmi1+* population contains also the proliferative cells of the central cornea (Supporting Information Fig. 4A-B''). In addition, we used BrdU incorporation to visualize the proliferative cells in the central cornea and limbus (Supporting Information Fig. 4D-E'). These observations reflected the brief maintenance of progenitors in the central cornea, where they are responsible for local, corneal renewal.

Bmi1+ cells are not proliferating during wound healing

We next performed an injury repair assay and chose to use an *in vivo* epithelial scraping wound instead of a chemical exposure. This approach removes only a selected region of the epithelium and leaves the rest of the epithelium unaffected, as opposed to chemical exposure, which in our hands affects most of the ocular surface, leaving no fully healthy regions for comparison. Importantly, we did not observe corneal opacification, neovascularization or conjunctivalization even 1 week after scraping (data not shown).

Repair after injury differs from homeostatic renewal in many organs. We assayed the role of *Bmi1+* progenitor cells in corneal wound healing after scraping the epithelium. *Bmi1* reporter expression was induced two weeks prior to wounding (Fig. 6A). As described above, we observed *Bmi1+* cell clusters in the central cornea, excluding the scraped region, immediately after wounding (Fig. 6B-B'). An epithelial wound was still visible 18 hours after injury (Fig. 6C), but genetic fate mapping of *Bmi1+*

cells did not reveal a pattern that differed from homeostasis (Fig. 6C'). By 72 hours, the epithelial wound had closed fully (Fig. 6D). This was confirmed by the genetic fate mapping; cell clusters appeared in central, peripheral and limbal cornea, suggesting a full closure of the wound, followed by a restoration of normal renewal (Fig. 6D'). Interestingly, we did not observe any modifications of the *Bmi1+* cell progeny patterning. In addition, we performed a similar epithelial wounding experiment without the inducible genetic fate mapping (Supporting Information Fig. S5A). In line with Fig. 6A, this assay indicated that injury did not induce accelerated cell proliferation (Supporting Information Fig. S5B). In search for possible alternative wound healing mechanisms, we studied the morphology of the epithelium in the proximity of the wound. We showed that 18 hours after injury the epithelium was markedly thinner in a region that expanded from the healthy peripheral cornea to the wound edge (Fig. S7A-B). This region only contained the basal and first suprabasal cells and lacked the superficial cells. However, 72 hours after wounding the cornea was healed (Fig. S7D). These observations hinted towards a possible cell intercalation and convergence extension as swift mechanism to heal the cornea after epithelial scraping.

Discussion

The mouse cornea is a fitted tool to study epithelial stem cells. Several groups showed that the corneal stem cells reside in the limbus [5–8]. Postnatal corneal epithelium renews itself locally, apparently without limbal input, until approximately 5 weeks of age [5,6]. In this study, we took a close focus on corneal maturation and renewal pattern from birth to adulthood. We identified *Bmi1* as a progenitor marker, which is excluded from the corneal epithelial stem cells, but expressed in the proliferating cells of the basal layer of the central cornea.

Like several other mammals, the mouse also has closed eyelids at the time of birth and the opening happens at about P14. During this period, the eye continues to grow and mature. In our study, we found evidence that the eyeball and cornea follow dissimilar patterns of growth; cornea grows markedly longer than the eyeball. This difference in growth is largely explained by the fact that the cornea covers only a small region of the ocular surface at birth, however by adulthood, it encapsulates almost half of the eyeball. Unlike in the human cornea, where proliferative cells localize from all corneal regions to limbus during a gestational maturation [26], we did not detect any changes in the distribution of *Ki67+* cells during the maturation process in mouse. Our analysis showed that the amount of *Ki67+* cells was always fitted to cornea size, so that tissue growth was coupled with a steady increase of *Ki67+* cells, but stayed in the same proportional level at all ages when adjusted to the size.

Previous reports have shown a late timeline for corneal maturation in the molecular level. *Krt14* expression progressively moves away from all epithelial layers to the basal cells of the central cornea and limbus at P10 [31]. In addition, α9β1 integrin expression moves from the central cornea to limbus by 8 weeks of age [32]. Thus, the limbal location of naïve epithelial cells is supported by the expression of these markers. In addition, the differentiation marker KRT12 covers fully the central cornea relatively late in mouse, by 12 weeks of age [31]. The mature and differentiated *Krt12+* cells

were present in the entire central corneal epithelium only by P90 [8]. Strikingly, the chronology we obtained with *Krt19* expression is much shorter. This differential timeline indicates that the populations labelled by these Keratins are separate. *Krt19+* cells are more naïve, and therefore *Krt19* expression disappears during cell differentiation in the cornea. We propose that *Krt12* expression could represent the last step of differentiation. In the light of our work, we propose that the limbal niche is defined before the terminal differentiation of the central cornea. Collectively, our results demonstrate that cell proliferation and cornea growth mirrored the molecular maturation of the cornea.

Genetic fate mapping provides a powerful tool to study tissue renewal. Up to date, no other marker than *Krt14* has been used to genetically fate map a restricted corneal cell population [7,8]. While *Bmi1* expression was demonstrated in the human limbus [11], the basal cell layer of the central mouse cornea contains mainly *Bmi1+* cells. Therefore, it is possible that the roles of *Bmi1* are different in human and mouse. Our genetic fate mapping and label retaining experiments show that the murine *Bmi1+* cells are not stem cells, but progenitors with a defined life-span. We analyzed the lifetime of *Bmi1+* cell clusters and illustrated that they maintained the central corneal epithelium for 4-8 weeks after induction. This time reflects the maximum length of the central corneal turnover time that is driven by the basal *Bmi1+* cells. This is clearly longer than was postulated in an earlier study, where progenitors exhibited a rapid turnover rate and long-living progenitors, like the *Bmi1+* progenitors, were not detected in the central cornea after 6 weeks [4]. However, our data is in line with a more recent observation, where central corneal patches were detectable even after 8-10 weeks from induction of a ubiquitous reporter expression [6]. When we analyzed 24 weeks old animals, we saw a low incidence of *Bmi1+* cell clusters compared to younger animals, indicating that tissue renewal from the *Bmi1+* cells had slowed down. One explanation is that at 24 weeks the central cornea is fully dependent on limbal input for tissue homeostasis. However, proliferative cells were present in the central cornea at 24 weeks, suggesting of regular cell divisions in the basal layer of the central

cornea. Another possibility is that the recombination efficiency is lower at 24 weeks compared to 4 weeks. *Bmi1* marks efficiently the central corneal progenitors cells in the young, but not in the mature murine cornea.

We challenged the capacity of the *Bmi1+* cells by inflicting an abrasion injury to the ocular surface. Majo et al., showed that large areas of the cornea can heal without limbal input and this is supported by evidence from LSC deficiency patients, who can maintain clear islets on the central cornea over a very long follow-up period [13,33]. On the other hand, upon chemical burn injury the LSCs are activated, but the extent of limbal input varies [4,7]. These results suggest that both central and limbal epithelial cells are responsive to ocular surface injury, possibly exerting different roles in the process of wound healing. After scraping the epithelium, the cornea healed fully within 72 hours, as reported earlier [34], but we could not detect a change in the *Bmi1+* cell progeny patterning. We detected a change in epithelial thickness at 18 hours after injury that corresponds to the most active period of healing. We propose that modifications in the organization of the epithelial layers, instead of proliferation, is the mode of healing after scraping injury. After loss of all epithelial cells in a large region of the cornea, only the basal (*Bmi1+*) and first suprabasal layers are constructed at first and only after that stratification begins and leads to full repopulation of all the epithelial cell layers, as our genetic fate mapping suggested. Interestingly, a similar mechanism, based on cell motility instead of proliferation, leading to cellular intercalation and convergent extension was shown to be responsible for the eyelid closure in embryonic mice [34]. Finally, our cell proliferation analysis rules out an extensive LSC activity after epithelial scraping.

Collectively, our results reflected a non-stem cell oriented role for BMI1. Because of the constant exposure of cornea to oxidative stress, and as *Bmi1* was shown to be involved in the maintenance of redox balance [35], we hypothesized that it could be an important function in the cornea as well. We believe that a further analysis of *Bmi1+* and negative cells can open up avenues to study the dynamic process of epithelial renewal in cornea. Perhaps corneal cells maintain an intricate hierarchy between

different stem cell and progenitor populations and these cells function in separate, but important processes and might exhibit redundancy.

Conclusions

Our experiments support the existence of central corneal progenitor cells and reveals that these progenitors maintain the corneal epithelium for a significant and limited time period, 4-8 weeks in young mice. We introduce Bmi1 as a marker for these progenitor cells. Our analysis suggests as well, that the cornea of a young mouse contains naïve cells that will locate to the limbus by the end of corneal maturation. Epithelial scraping wounds showed that the Bmi1+ cells maintain central turnover rate at a regular pace during wound healing via epithelial reorganization.

References

1 Zieske JD. Corneal development associated with eyelid opening. Int J Dev Biol 2004;48:903–911.

2 Schermer A, Galvin S, Sun TT. Differentiation-related expression of a major 64K corneal keratin in vivo and in culture suggests limbal location of corneal epithelial stem cells. J Cell Biol 1986;103:49–62.

3 Cotsarelis G, Cheng S-Z, Dong G, et al. Existence of slow-cycling limbal epithelial basal cells that can be preferentially stimulated to proliferate: Implications on epithelial stem cells. Cell 1989;57:201–209.

4 Lehrer MS, Sun TT, Lavker RM. Strategies of epithelial repair: modulation of stem cell and transit amplifying cell proliferation. J Cell Sci 1998;111.

5 Collinson JM, Morris L, Reid AI, et al. Clonal analysis of patterns of growth, stem cell activity, and cell movement during the development and maintenance of the murine corneal epithelium. Dev Dyn 2002;224:432–440.

6 Dorà NJ, Hill RE, Collinson JM, et al. Lineage tracing in the adult mouse corneal epithelium supports the limbal epithelial stem cell hypothesis with intermittent periods of stem cell quiescence. Stem Cell Res 2015;15:665–677.

7 Amitai-Lange A, Altshuler A, Bubley J, et al. Lineage Tracing of Stem and Progenitor Cells of the Murine Corneal Epithelium. Stem Cells 2015;33:230–239.

8 Di Girolamo N, Bobba S, Raviraj V, et al. Tracing the Fate of Limbal Epithelial Progenitor Cells in the Murine Cornea. Stem Cells 2015;33:157–169.

9 Pan YA, Freundlich T, Weissman TA, et al. Zebrabow: multispectral cell labeling for cell tracing and lineage analysis in zebrafish. Development 2013;140.

10 Potten CS. The epidermal proferative unit: the possible role of the central basal cell. Cell Prolif 1974;7:77–88.

11 Barbaro V, Testa A, Di Iorio E, et al. C/EBPδ regulates cell cycle and self-renewal of human limbal stem cells. J Cell Biol 2007;177:1037–1049.

12 Levis HJ, Daniels JT. Recreating the Human Limbal Epithelial Stem Cell Niche with Bioengineered Limbal Crypts. Curr Eye Res 2016;41:1153–1160.

13 Majo F, Rochat A, Nicolas M, et al. Oligopotent stem cells are distributed throughout the mammalian ocular surface. Nature 2008;456:250–254.

14 Park I, Qian D, Kiel M, et al. Bmi-1 is required for maintenance of adult self-renewing haematopoietic stem cells. Nature 2003;423:302–305.

15 Iwama A, Oguro H, Negishi M, et al. Enhanced Self-Renewal of Hematopoietic Stem Cells Mediated by the Polycomb Gene Product Bmi-1. Immunity 2004;21:843–851.

16 Molofsky A V., Pardal R, Iwashita T, et al. Bmi-1 dependence distinguishes neural stem cell self-renewal from progenitor proliferation. Nature 2003;425:962–967.

17 Sangiorgi E, Capecchi MR. Bmi1 is expressed in vivo in intestinal stem cells. Nat Genet 2008;40:915–920.

18 Biehs B, Hu JK-H, Strauli NB, et al. BMI1 represses Ink4a/Arf and Hox genes to regulate stem cells in the rodent incisor. Nat Cell Biol 2013;15:846–852.

19 Yan KS, Chia LA, Li X, et al. The intestinal stem cell markers Bmi1 and Lgr5 identify two functionally distinct populations. Proc Natl Acad Sci U S A 2012;109:466–471.

20 Van Der Lugt NMT, Domen J, Linders K, et al. Posterior transformation, neurological abnormalities, and severe hematopoietic defects in mice with a targeted deletion of the bmi-1 proto-oncogene. Genes Dev 1994;8:757–769.

21 López-Arribillaga E, Rodilla V, Pellegrinet L, et al. Bmi1 regulates murine intestinal stem cell proliferation and self-renewal downstream of Notch. Development 2014;142:41–50.

22 Liu J, Cao L, Chen J, et al. Bmi1 regulates mitochondrial function and the DNA damage response pathway. Nature 2009;459.

23 Soriano P. Generalized lacZ expression with the ROSA26 Cre reporter strain. Nat Genet 1999;21:70–71.

24 Pispa J, Pummila M, Barker PA, et al. Edar and Troy signalling pathways act redundantly to regulate initiation of hair follicle development. Hum Mol Genet 2008;17:3380–3391.

25 Echevarria TJ, Girolamo N Di. Tissue-Regenerating, Vision-Restoring Corneal Epithelial Stem Cells. Stem Cell Rev Reports 2010;7:256–268.

26 Lauweryns B, Van den Oord JJ, Missotten L. The transitional zone between limbus and peripheral cornea: An immunohistochemical study. Investig Ophthalmol Vis Sci 1993;34:1991–1999.

27 Kasper M, Moll R, Stosiek P, et al. Patterns of cytokeratin and vimentin expression in the human eye. Histochemistry 1988;89:369–377.

28 Yoshida S, Shimmura S, Kawakita T, et al. Cytokeratin 15 Can Be Used to Identify the Limbal Phenotype in Normal and Diseased Ocular Surfaces. Investig Opthalmology Vis Sci 2006;47:4780.

29 Davies SB, Chui J, Madigan MC, et al. Stem Cell Activity in the Developing Human Cornea. Stem Cells 2009;27:2781–2792.

30 Brocard J, Warot X, Wendling O, et al. Spatio-temporally controlled site-specific somatic mutagenesis in the mouse. Proc Natl Acad Sci U S A 1997;94:14559–14563.

31 Tanifuji-Terai N, Terai K, Hayashi Y, et al. Expression of keratin 12 and maturation of corneal epithelium during development and postnatal growth. Investig Ophthalmol Vis Sci 2006;47:545–551.

32 Pajoohesh-Ganji A, Ghosh SP, Stepp MA. Regional distribution of ?9?1 integrin within the limbus of the mouse ocular surface. Dev Dyn 2004;230:518–528.

33 Dua HS, Miri A, Alomar T, et al. The Role of Limbal Stem Cells in Corneal Epithelial Maintenance. Ophthalmology 2009;116:856–863.

34 Heller E, Kumar KV, Grill SW, et al. Forces generated by cell intercalation tow epidermal sheets in mammalian tissue morphogenesis. Dev Cell 2014;28:617–632.

35 Yin Y, Xue X, Wang Q, et al. Bmi1 plays an important role in dentin and mandible homeostasis by maintaining redox balance. Am J Transl Res 2016;8:4716–4725.

Figure Legends

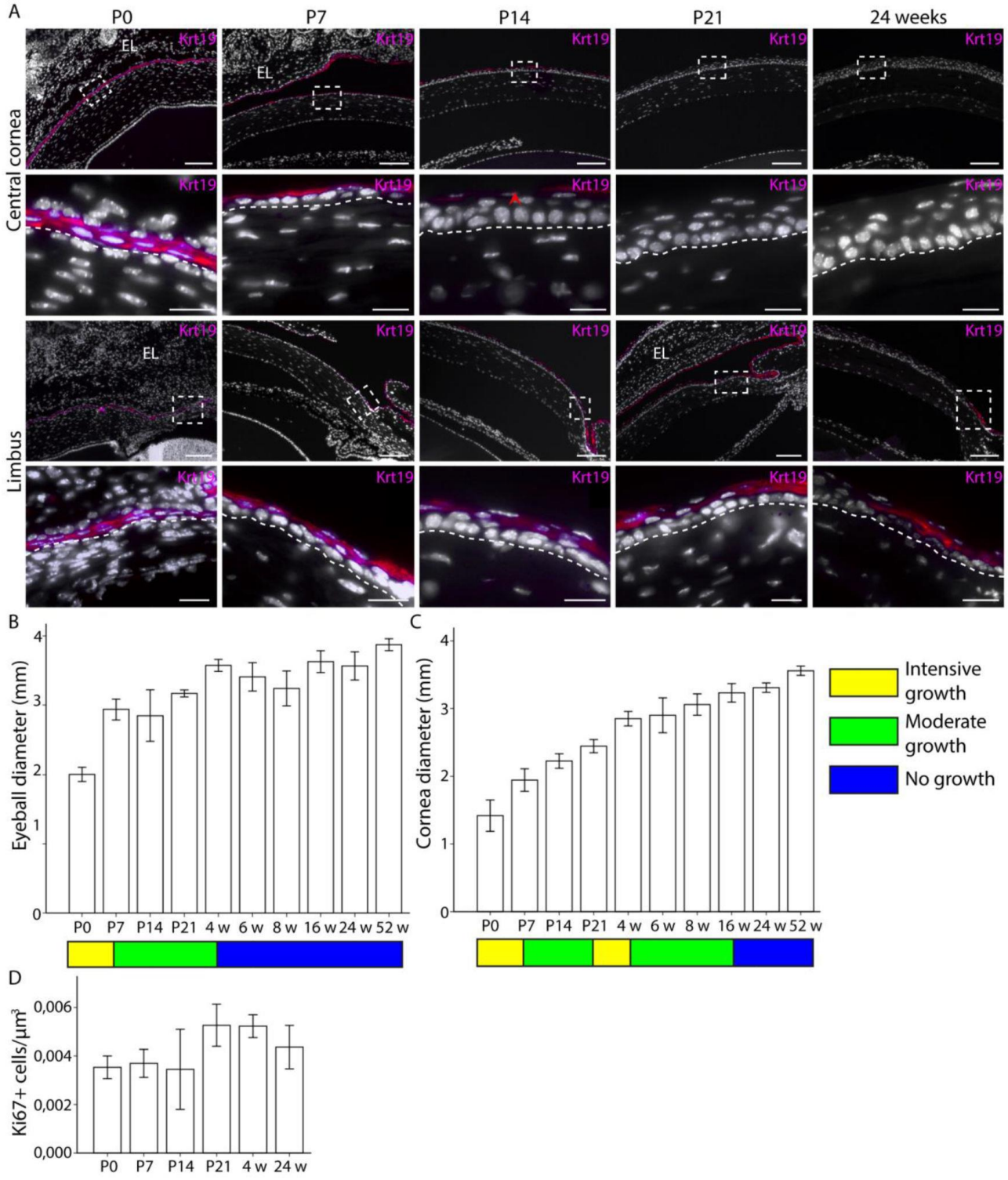

Figure 1.

Krt19 expression pattern correlates with cornea growth and maturation. Krt19 expressing cells are marked with magenta. **(A)**: At P0, all corneal epithelial cells were Krt19+. Boxes indicate the location of insets. At P7, the expression domain excluded the basal cells in the central and limbal cornea. The border between epithelium and stroma is marked with a

dashed line. By P14, the central corneal epithelial cells were almost all Krt19-negative (arrowhead), but the limbal epithelial cells were Krt19+. At P21, we could not detect Krt19 expression in the central cornea anymore, in contrast to noticeable expression in the limbus. After that the expression pattern remained constant; at 24 weeks of age the limbal epithelial cells were Krt19+. However, signal from the central and peripheral cornea was completely lost. **(B-C)**: Growth rate is indicated with a color pattern: yellow for intensive growth, green for moderate growth and blue for no more growth. **(B)**: Eyeball diameter increased quickly from P0 until P7 ($p=0.000$), then with moderate pace from P7 until 4 weeks ($p=0.000$); after that growth ceased ($p \geq 0.474$). **(C)**: Cornea diameter increased stepwise between P0 and P7 ($P=0.000$) as well as between P21 and 4 weeks ($p=0.005$), with periods of moderate growth ($p=0.000$) after each quick growth phase. Cornea diameter did not increase anymore after 16 weeks of age ($p \geq 0.193$). **(D)**: The amount proliferating, Ki67+ cells were steadily maintained in an appropriate level at each age ($p \geq 0.125$). Errors bars indicate 2 ± standard error. Hoechst for nuclear staining (white). Eyelid (EL). Scale bars are 100 μm, 20 μm for insets.

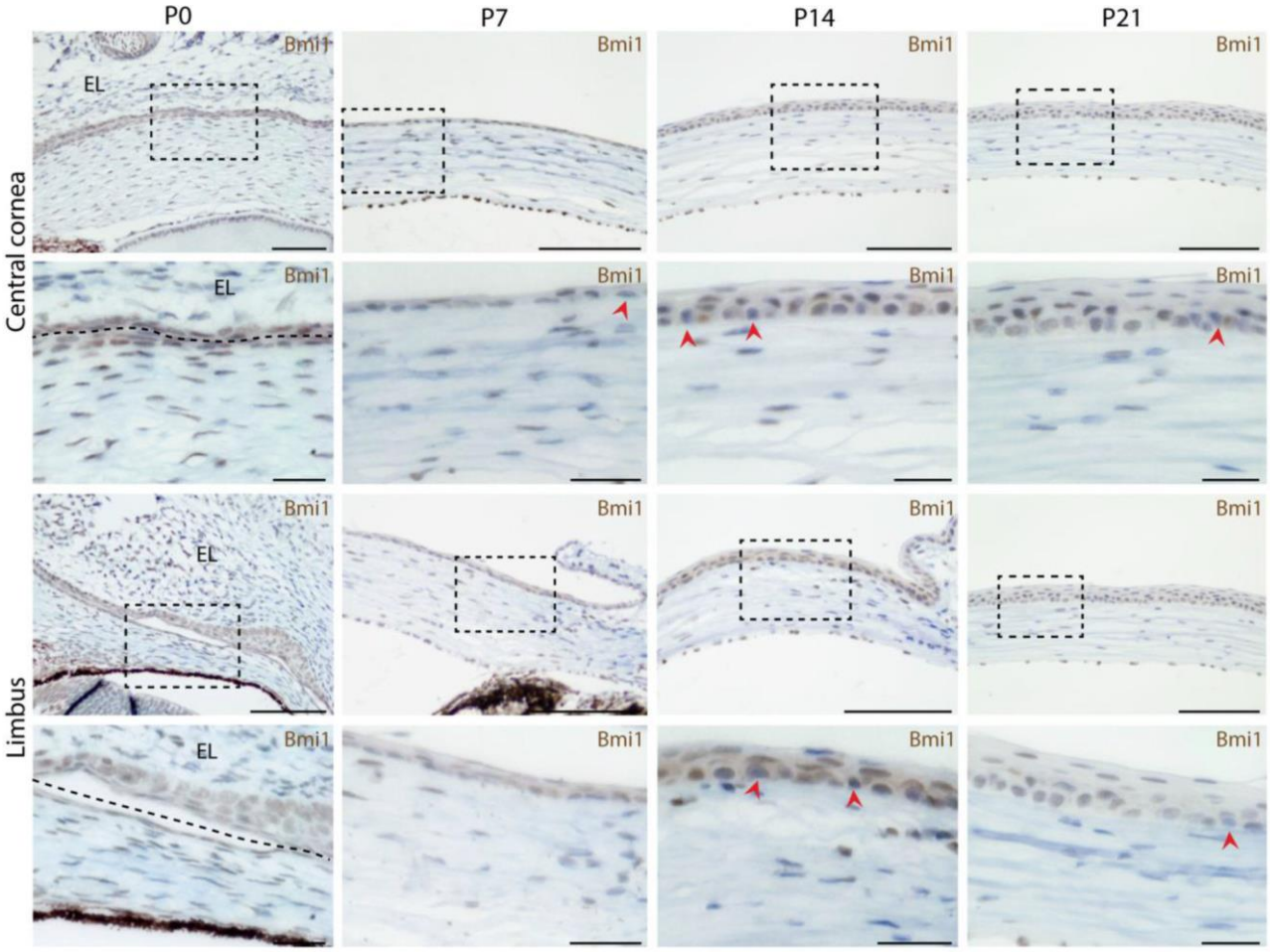

Figure 2.

Bmi1 expression is steady during cornea maturation. BMI1 immunostaining in brown. Bmi1 is expressed throughout both epithelial layers before epithelial stratification begins (boxes show the location of insets). The border between corneal epithelium and inner eyelid is marked with a dashed line. P14 marks the beginning of eyelid opening and epithelial stratification. Bmi1 is mostly expressed in the basal epithelium, but visible also in the suprabasal epithelium. All layers contain some Bmi1-negative cells (arrowheads). At P21 Bmi1 becomes more confined to the basal epithelium, however, rare Bmi1-negative cells remain as well as some Bmi1+ in the suprabasal layer. Hematoxylin for nuclear staining (blue). Scale bars are 100 μm, 25 μm for the insets.

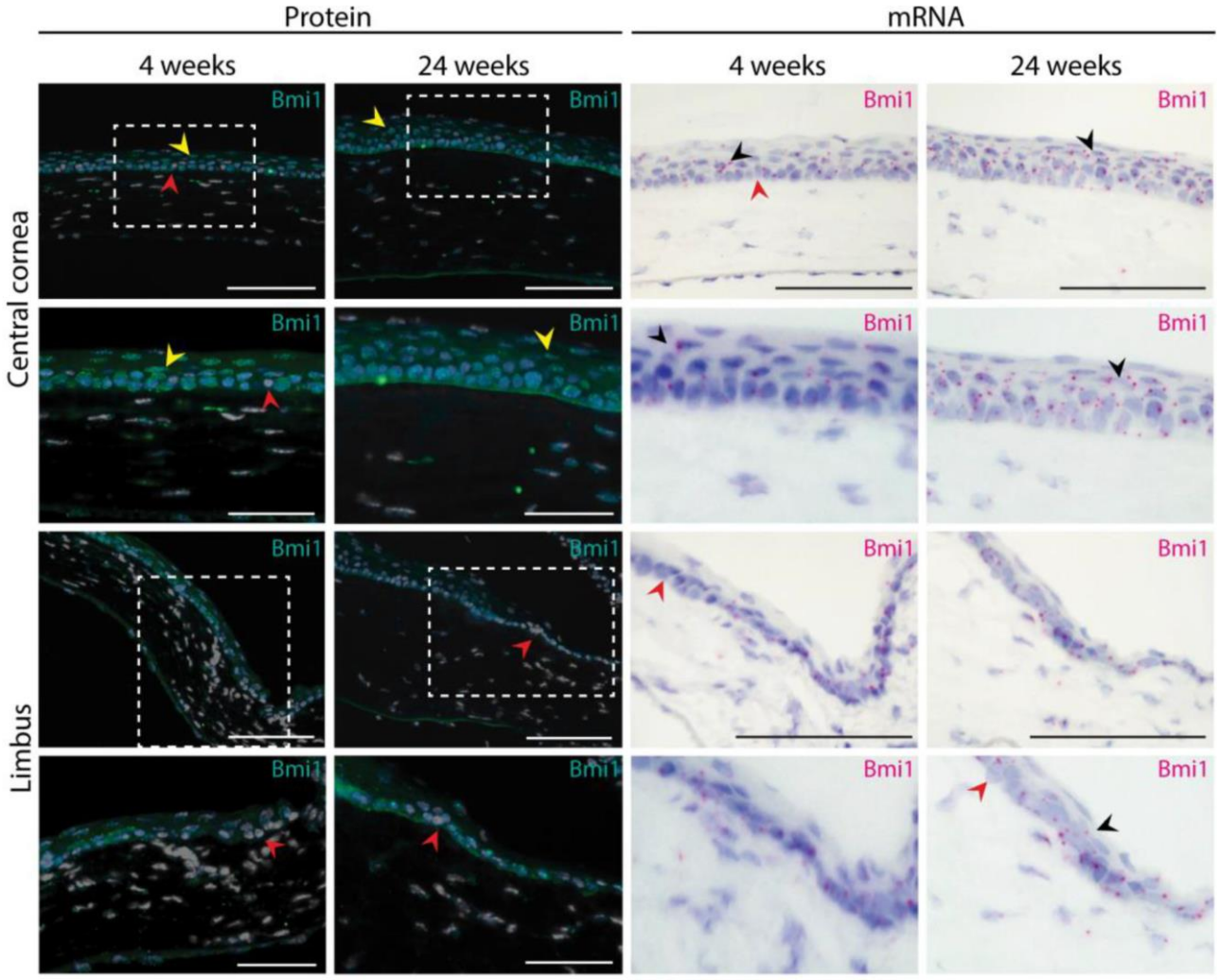

Figure 3.

Bmi1 expression pattern remains unchanged after cornea maturation. We assayed both BMI1 protein (in turquoise) and Bmi1 RNA (in magenta). Young (4 weeks old) and adult mice (24 weeks old) displayed the same expression pattern. Most of the epithelial basal cell layer of the cornea was composed of Bmi1+ cells. In both stages, we discovered few Bmi1-negative cells in the basal layer (red arrowhead). Some suprabasal cells expressed Bmi1 in the adult cornea (yellow or black arrowhead). Hoechst for nuclear staining (white) and hematoxylin for nuclear staining (blue). Scale bars are 100 μm, 50 μm for the insets.

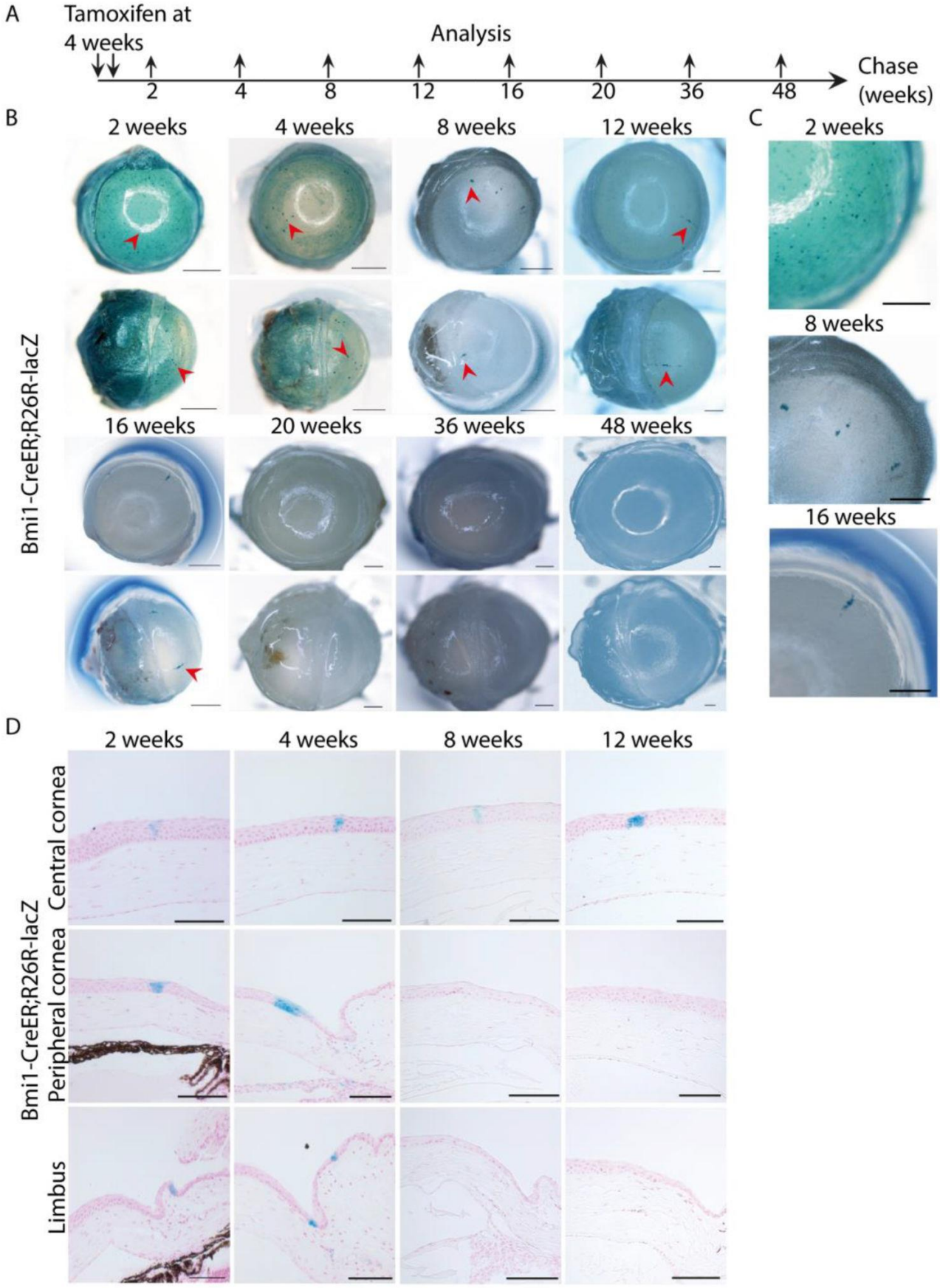

Figure 4.

Genetic fate mapping of Bmi1+ cells reveals progenitor-like dynamics. (A): Schematic drawing of the genetic fate mapping experiment. The recombinase was induced at 4 weeks of age and eyeballs were regularly collected after 2 to 48

weeks of chase. (B): Bmi1+ cells and their progeny are marked in blue due to LacZ expression. The bright ring on top of the central cornea is a technical artefact from the camera. For each time point, we sacrificed 3 littermates and chose a representative image to showcase. After 2 and 4 weeks post-induction, blue cell clusters emerged in the central, peripheral and limbal cornea (arrowheads). Between 8 and 16 weeks of chase, these clusters gradually disappeared, leaving few stripes visible (arrowheads). We did not note any progeny from 20 weeks onwards. (C): Insets of cornea after 2, 8 and 16 weeks of chase. (D): The histological sections confirmed that Bmi1+ cells and their progeny formed columnar clones within the epithelium in the central, peripheral and limbal cornea after short chases. Nuclear FAST red for nuclear staining (red). Scale bars are 1 mm (B-C) and 100 μm (D).

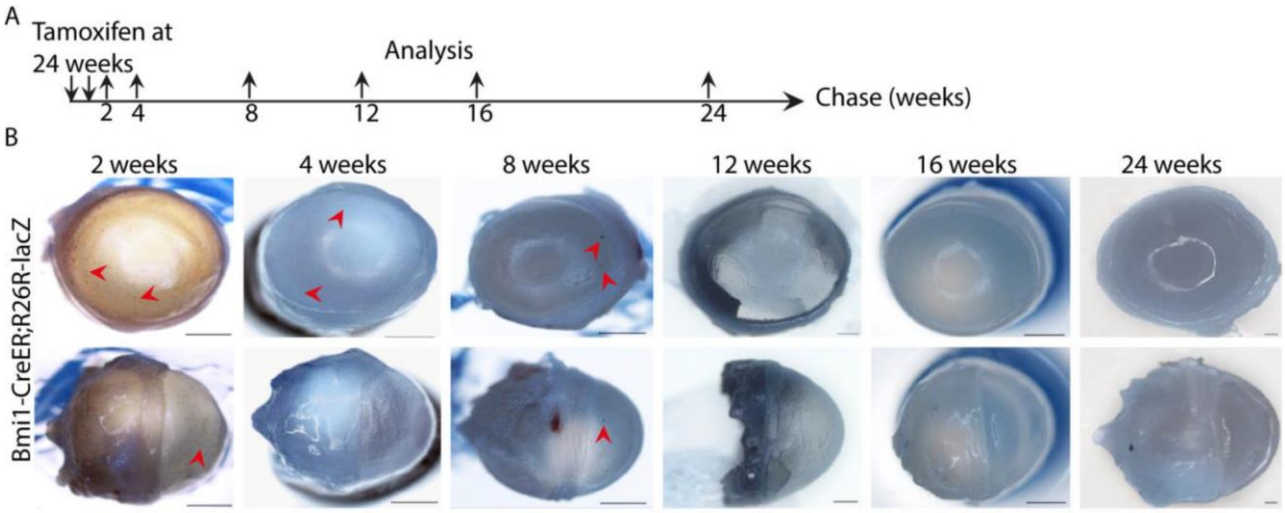

Figure 5.

Genetic fate mapping of Bmi1+ cells shows short-lived clones in fully mature mice. (A): Schematic drawing of the genetic fate mapping experiment. The recombinase was induced at 24 weeks of age and eyeballs were regularly collected after 2 to 24 weeks of chase. (B): We observed Bmi1+, rare clusters in the cornea after 2, 4 and 8 weeks of chase (arrowheads). After 12 weeks of chase, Bmi1+ cells did not produce new progeny. Scale bars are 1 mm.

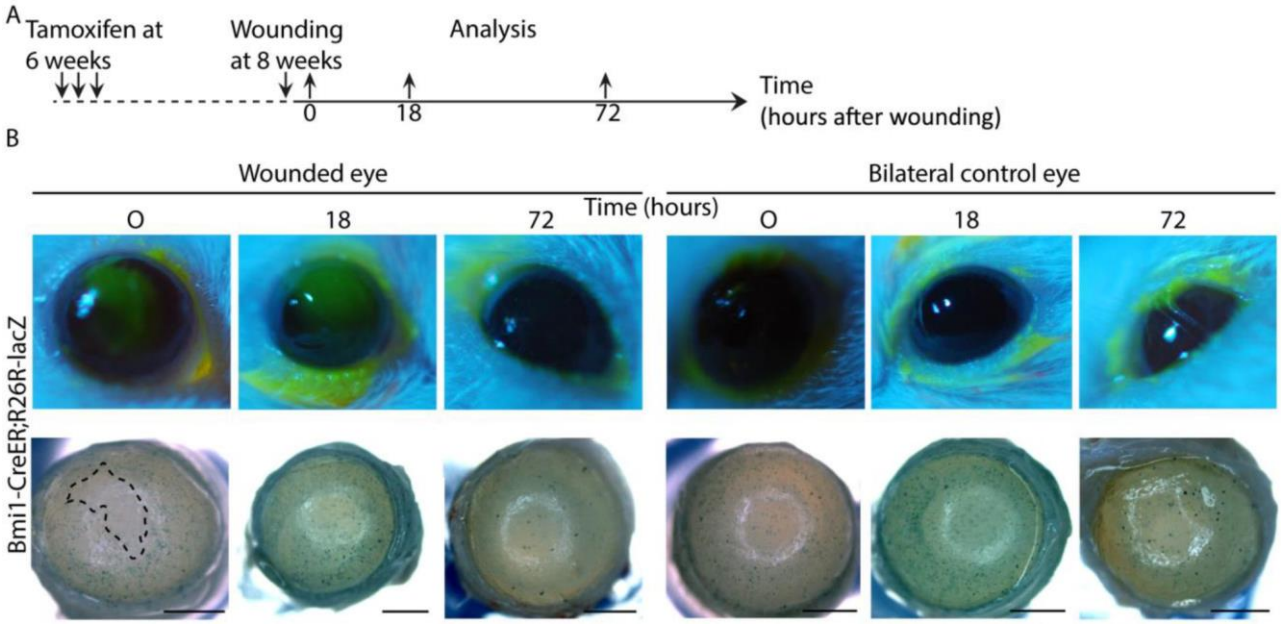

Figure 6.

Corneal wounding reveals that Bmi1+ cells are not proliferative upon injury. (A): LacZ expression was induced at 6 weeks in Bmi1CreERT/wt;R26RLacZ/wt mice, followed by a scraping wound 2 weeks later on one eye/animal. We collected both eyes immediately after wounding, 18 hours or 72 hours after. For each time point, we sacrificed 3 littermates and chose a representative image to showcase. (B): Fluorescein staining in green shows the wounded region and an area devoid of cells, e.g. the wounded area, is marked with a dashed line in the lower panel. The wound is still clear after 18 hours, but fate mapping shows a normal, patchy pattern outside the wounded region. By 72 hours after wounding, the cornea is fully healed and central renewal pattern follows a regular pattern. Right panels show the bilateral, unwounded control eye at each time point. Scale bar is 1 mm.

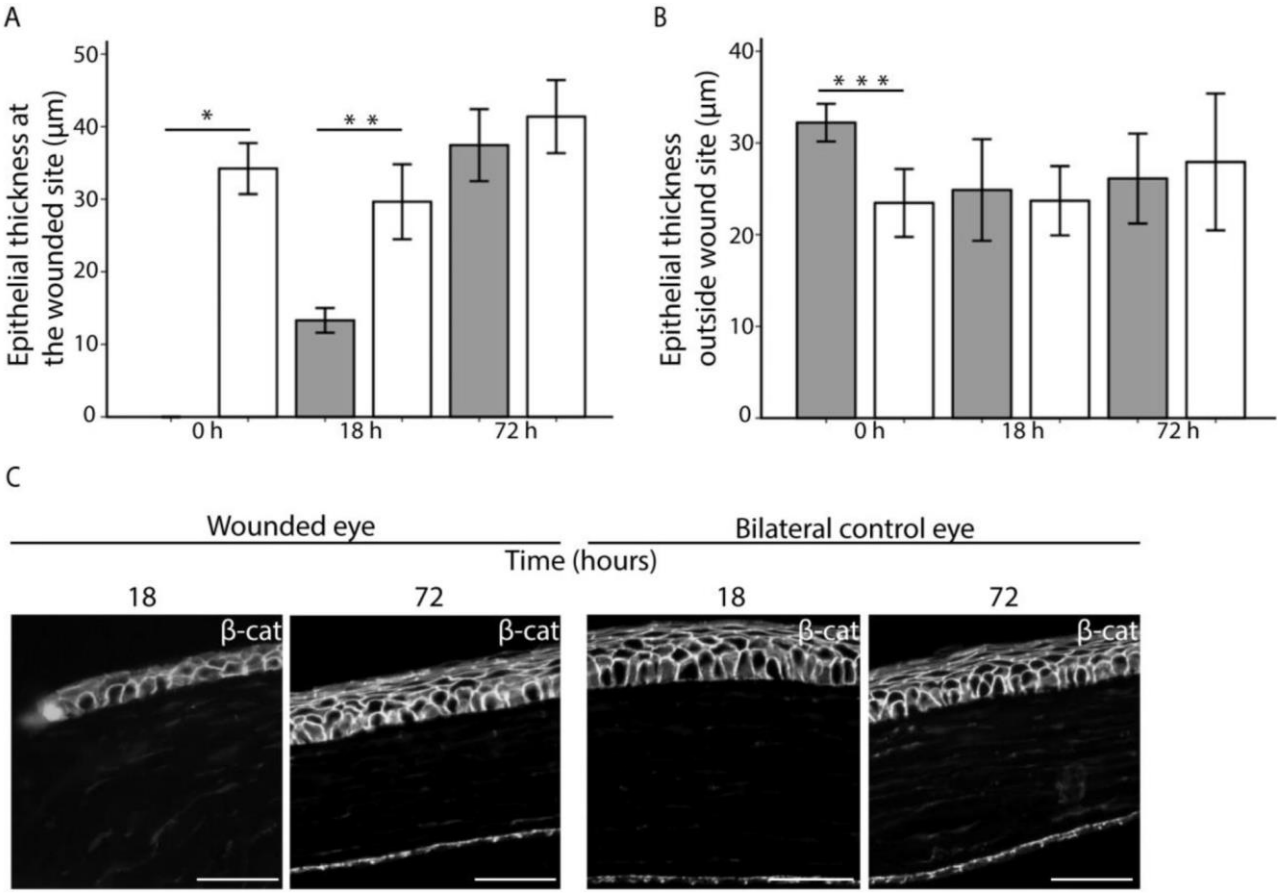

Figure 7.

Epithelial thickness changes during wound healing. (A): Estimation of epithelial thickness 0, 18 and 72 hours post injury in the center of the cornea (grey bars). Control samples (white bars) represent the thickness of the epithelium in the bilateral, unwounded eyes in a similar location. The epithelium was significantly thinner in the cornea 0 hours ($p=0.000$) and 18 hours ($p=0.001$) after injury. (B): Thickness of the epithelium in peripheral cornea after 0, 18 and 72 hours post injury. The control epithelium was significantly thinner at 0 hours ($p=0.002$), which might reflect retraction of the epithelium due to loosened mechanimal forces just after abrasion. At other time points, epithelium was not thinner in the abrased cornea compared to the control. (C): The re-epithelializing zone 18 hours after injury consists of only two epithelial cell layers. Epithelium has recovered at 72 hours. Unwounded control eyes. β-catenin (in white) shows cell borders. Scale bar is 50 µm. Error bars indicate 2 ± standard error.